



Exploring impacts of forest management strategies on water partitioning in a drought-sensitive catchment using a tracer-aided ecohydrological framework

Cong Jiang¹, Doerthe Tetzlaff^{1,2,3}, Songjun Wu¹, Christian Birkel^{1,4}, Hjalmar Laudon⁵, and Chris Soulsby^{1,3,5,6}

¹Department of Ecohydrology and Biogeochemistry, Leibniz Institute of Freshwater Ecology and Inland Fisheries (IGB), Berlin, Germany

²Department of Geography, Humboldt University Berlin, Berlin, Germany

³Northern Rivers Institute, University of Aberdeen, Aberdeen, UK

⁴Department of Geography, University of Costa Rica, San Pedro, Costa Rica

⁵Department of Forest Ecology and Management, Swedish University of Agricultural Science (SLU), Umeå, Sweden

⁶Chair of Water Resources Management and Modeling of Hydrosystems, Technical University Berlin, Berlin, Germany

Correspondence: Cong Jiang (cong.jiang@igb-berlin.de)

Received: 30 May 2025 – Discussion started: 26 June 2025

Revised: 27 May 2026 – Accepted: 4 June 2026 – Published: 22 June 2026

Abstract. Land use strongly influences water partitioning, water availability, and ecohydrological resilience in drought-sensitive regions. Forest management plays a critical role through its effects on water use, which depends on forest type, forest density, root water uptake, yet the ecohydrological consequences of different forest management strategies – particularly in terms of blue and green water fluxes – remain poorly quantified. Here, we develop and apply a parsimonious, tracer-aided forest management scenario framework using the conceptual ecohydrological model EcoPlot-iso, designed to isolate the dominant vegetation-structural controls on long-term water partitioning. We investigated how variations in generic forest type (e.g., broadleaf vs. conifer), forest density, and root distribution influence water partitioning and ecohydrological resilience under different wetness conditions in the drought-sensitive lowland Demnitzer Millcreek catchment (DMC), northeastern Germany. Baseline simulations for the period 2000–2024 were conducted at three forest sites and used to develop forest-type-specific reference conditions for comparison with alternative forest management scenarios. A key innovation in this version of EcoPlot-iso was the integration of a depth-dependent root water uptake function, allowing simulation of transpiration across soil layers under contrasting rooting distributions corresponding to different stand ages. The model was calibrated and validated

using seven years of soil moisture and three years of soil water isotope ($\delta^2\text{H}$) data through a multi-criteria approach. Results showed that, on average, evapotranspiration was highest under conifers, exceeding broadleaf forests and agroforestry by 7% and 11%, respectively, while agroforestry exhibited the greatest groundwater recharge. Significant differences in water partitioning between dry and wet years were observed across management scenarios. Conifer forests showed stronger transpiration contrasts than broadleaf forests in early spring, while the wet–dry-year contrast between the two forest types was largest in late spring. Our findings highlight the potential of agroforestry, such as crop–tree mixtures, to mitigate drought impacts on soil water availability and groundwater recharge. Overall, this study demonstrates how a parsimonious, tracer-aided scenario framework can be used as a decision-support tool to quantify and visualize the effects of land use change on water availability in data-limited regions, supporting more informed decision-making and enhanced ecohydrological resilience under increasing drought pressure.

1 Introduction

Land use plays a crucial role in regulating water, carbon, energy, and nutrient cycles by mediating ecohydrological fluxes and soil water storage dynamics which link interactions between the atmosphere, soils, vegetation and biogeochemical processes (Mahmood et al., 2014; Pielke et al., 2011; Smith et al., 2021; Sterling et al., 2013). Among the different types of land cover, forests are particularly important elements of the land use mosaic, providing a range of ecosystem services, including enhancing infiltration, stabilizing soils, storing carbon, supplying timber and fuelwood, as well as buffering extreme climate events (Bonan, 2008). However, there are clear trade-offs, as forests and trees also tend to use more water than contrasting land uses (Bosch and Hewlett, 1982; Calder, 1998). This is because their high Leaf Area Index (LAI) and canopy storage capacities often result in greater interception losses and canopy evaporation, while their deeper and denser rooting networks can sustain transpiration when top soils dry out (Wang-Erlandsson et al., 2014). Consequently, forest management decisions (e.g., afforestation, thinning, and forest type selection) can significantly affect water yield and the partitioning into blue water fluxes (runoff and groundwater recharge) and green water fluxes (evapotranspiration), as well as the ecohydrological resilience to drought. Here, ecohydrological resilience is defined as the ability of the soil–plant–water system to maintain key ecohydrological functions, including soil moisture storage, transpiration, and groundwater recharge, under drought stress (Falkenmark and Rockström, 2006; Neill et al., 2021; Tetzlaff et al., 2024).

Sustainable land management also requires consideration of sensitivity to climate change, which is altering hydroclimatic regimes by shifting precipitation patterns and increasing atmospheric moisture demand (Huntington, 2006; Trenberth, 2011). These changes can intensify drought frequency and duration, increase evaporative losses, and reduce groundwater recharge and surface water availability, thereby exacerbating water scarcity in many regions (Ault, 2020; Yuan et al., 2023). Because land use practices – particularly forest management – are expected to strongly influence water partitioning, it is important to assess their impacts under changing hydroclimatic conditions in order to evaluate the ecohydrological resilience of soil–plant–water systems, especially in drought-sensitive areas.

The understanding of how land use change affects runoff generation, soil moisture storage and evapotranspiration dynamics has gradually developed through decades of research, including long-term paired experimental watershed investigations of water yield (Bosch and Hewlett, 1982; Brown et al., 2005, 2013; Hibbert, 1967). However, quantifying the impact of forest management on water partitioning remains challenging in most situations (Guswa et al., 2020). This is due to the complex interplay of climate conditions, soil properties, vegetation type, and topography, and the difficulty

in distinguishing individual evapotranspiration (ET) components (Kool et al., 2014; Smith et al., 2021; Zhang et al., 2001). These challenges are further compounded by scarce long-term observational data for forest ecosystems, which are essential given their slow dynamics and lengthy growth cycles (Tetzlaff et al., 2017).

In forest ecosystems, ET is particularly challenging to simulate due to complex interactions among canopy structure, stomatal behavior, and root water uptake (Tague and Band, 2004). Many ecohydrological models include some form of root water uptake parameterization (e.g., mHM, Ech2O-iso, RHESys), in which canopy transpiration is typically constrained by surface energy balance and stomatal conductance and subsequently distributed among soil layers based on soil water availability and root distribution. While such models provide detailed representations of land–atmosphere and soil–vegetation interactions, their application in forest management studies is often constrained by high data requirements, computational demand, and parameter uncertainty, particularly in data-scarce regions (Fatichi et al., 2012; Ricci et al., 2020; Tague and Band, 2004). In this context, conceptual tracer-aided ecohydrological models can provide a complementary, process-based, and practical framework for systematically exploring long-term forest management impacts on water partitioning and ecohydrological resilience (Landgraf et al., 2023). By integrating climatic forcing, canopy structure (e.g., leaf area index), soil moisture dynamics, and stable water isotopes, such approaches facilitate robust assessment of green- and blue-water fluxes under contrasting forest management scenarios (Neill et al., 2021).

In this study, we apply the tracer-aided conceptual model EcoPlot-iso to assess how land use, specifically forest management strategies, influences water partitioning and soil moisture storage in the drought-sensitive, lowland Demnitzer Millcreek catchment, NE Germany. This lowland catchment is typical of large areas in central Europe where freely draining, sandy soils combine with relatively low precipitation, and high evaporative demand amplify drought stress under climate change. To improve the quantification of transpiration, we introduce a novel development in EcoPlot-iso by integrating a depth-dependent root water withdrawal function into the transpiration equation. The model is dual-calibrated and validated using seven years of soil moisture data and three years of soil water isotope data. A series of generic forest management scenarios – varying broad forest types (broadleaf, coniferous, agroforestry), forest density, and rooting characteristics – are developed within a parsimonious, tracer-aided forest management scenario framework, to explore their impacts on vertical water fluxes and ecohydrological resilience.

This study aims to answer the following research questions:

- How does vegetation cover influence water use and partitioning under varying wetness conditions in a drought-sensitive, lowland catchment?
- What are the implications of alternative generic forest management scenarios for water availability and overall ecohydrological resilience?
- How can land management strategies be optimized to reduce drought impacts on soil water availability and groundwater recharge and enhance ecohydrological resilience under climate change?

2 Study area

2.1 Demnitzer Millcreek catchment (DMC)

The Demnitzer Millcreek catchment (DMC) is a 66 km² lowland basin (30–90 m elevation) in the State of Brandenburg, Germany, approximately 55 km east of Berlin (52°23' N, 14°15' E) (Fig. 1). Located in the Northern European Plain, it is part of a drought-sensitive region that provides many essential ecosystem services, including agriculture, timber production, and water supply.

The DMC landscape is dominated by non-irrigated farmland, mostly arable crops and some grazing on more water-retentive brown earth and gley soils respectively which cover 60 % of the catchment (Fig. 1a and b). Forests cover 36 % of the catchment on more freely draining sandy soils, and include coniferous, broadleaf, and mixed stands. Small urban settlements (2 %) are scattered throughout the catchment, with wetlands on peat soils primarily found along streams in the central part of the catchment. The climate is temperate with warm summers, with a mean annual temperature of 9.6 °C and average precipitation of approximately 558 mm, based on weather station data from 2000 to 2024. Potential evapotranspiration (PET) ranges from 584 to 789 mm per year from 2000 to 2024, based on calculations from this study (see Sect. 3.3). Interannual variability in precipitation, including the identification of dry and wet years, is shown in Fig. S1, which highlights deviations from the long-term mean and helps contextualize recent drought impacts. Rainfall peaks in summer, accompanied by intense convective storms; however, surface runoff is rare, as the soils are highly permeable and dry in the growing season. Consequently, the catchment is primarily groundwater-dominated with winter high flows and often dries in the summer (Smith et al., 2021). The geology consists mainly of glacial and fluvial deposits and base moraines, while the dominant soil types include poorly drained silty gley brown earth and well-drained podzolic brown earth soils (Fig. 1b).

The DMC has a long history of human influence, with significant land use changes affecting its hydrology. In the 18th Century, artificial drainage channels were constructed to convert wetlands into agricultural land. Since the 1990s, ef-

forts in wetland restoration and wildlife recolonization (e.g., beaver recovery) have aimed to enhance water retention in the landscape. Long-term hydrological and isotopic monitoring (Gelbrecht et al., 1996, 2005; Smith et al., 2020; Wu et al., 2021) has provided valuable insights into the impacts of agriculture and land use management on water quality, ecohydrological partitioning and soil water storage. The 2018 European drought and subsequent prolonged dry periods have exacerbated water scarcity and ecosystem vulnerability (Kleine et al., 2021). In response, some land owners have explored agroforestry and other adaptive forest and tree management strategies to improve water retention and reduce drought vulnerability (Luo et al., 2024). Agroforestry represents a transitional system blending low density tree cultivation with agriculture; either in terms of grazing the understory vegetation or crops (Landgraf et al., 2022; Quandt et al., 2023). Given the long-term monitoring record and ongoing land use change, DMC serves as a useful site for assessing the impacts of changing forest management on water partitioning, soil moisture and ecohydrological resilience under different wetness conditions.

2.2 Forest Plot Sites

To investigate the effects of forest management scenarios on water partitioning and ecohydrological resilience, three predominantly forest plot sites – broadleaf forest, conifer forest and agroforestry – were selected within the drought-sensitive DMC. These plots represent contrasting forest types central to the modelling experiments. The plot locations are shown in Fig. 1, and key site characteristics are summarized below, with further details available in Kleine et al. (2021) and Landgraf et al. (2023). A summary of observed soil types and soil moisture monitoring characteristics for these three forest sites is provided in Table 1, which also highlights pronounced differences in long-term mean volumetric soil moisture averaged over the 0–1 m soil profile, with values highest in agroforestry (~ 21 %), intermediate in broadleaf (~ 11 %), and lowest in conifer forest (~ 5.5 %).

The broadleaf forest site represents a relatively mature forest system (~ 60 years old) and is dominated by mature European oak (*Quercus robur*) with a few Scots pine (*Pinus sylvestris*) present within the plot. Additional species including Norway maple (*Acer platanoides*), elm (*Ulmus* spp.), and hazel (*Corylus avellana*) are found within 10 m of the plot boundary. The soil is classified as brown earth, with a loamy sand to sand texture.

The conifer forest site is structurally simpler and more homogeneous, and is dominated by mature Scots pine (*Pinus sylvestris*) plantation. A limited number of broadleaf species, such as European oak and Norway maple, are also present within the plot, reflecting a conifer-dominated canopy. The soil is a weakly developed brown earth, characterized by coarse sandy texture and overlying gravels.

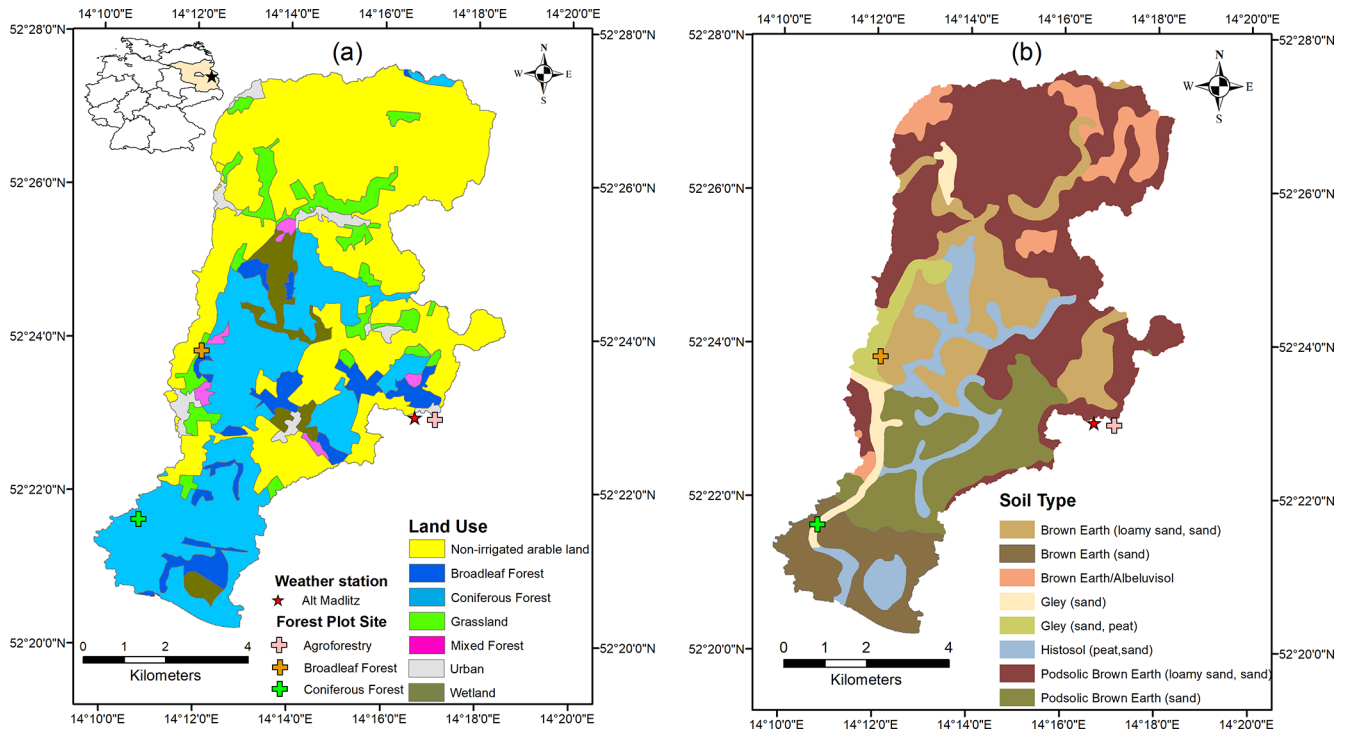


Figure 1. Location, land use (a) and soil type (b) map of the Demnitzer Millcreek catchment, showing the current distribution of broadleaf forests, conifer forests, agroforestry, cropland, and grassland.

The agroforestry site represents a transitional system between forest and agriculture and is characterized by minimal canopy cover and no irrigation. It consists of rows of small deciduous trees or shrubs (≤ 2 m in height), spaced approximately 2–3 m apart, interplanted with rainfed legumes (Landgraf et al., 2023). The soil is classified as podsolc brown earth, with a loamy sand to sand texture.

Together, these three sites represent a realistic gradient of forest land use intensity and provide a basis for exploring how forest type, forest density, and rooting depth affect ecohydrological responses under varying climatic conditions.

3 Method and Data

3.1 Model Framework and Structure

This study employs the EcoPlot-iso model, a tracer-aided ecohydrological modelling framework designed to simulate key ecohydrological and isotopic processes that characterise water partitioning at the plot scale (Birkel et al., 2024; Landgraf et al., 2023; Stevenson et al., 2023). EcoPlot-iso is a process-based conceptual model that simulates key ecohydrological fluxes, including interception, throughfall, infiltration, preferential flow, surface runoff, percolation, and groundwater recharge, as well as evapotranspiration components such as canopy evaporation, soil evaporation, and transpiration (Fig. 2a). These processes are represented within a

vertical structure comprising a single canopy layer and three soil layers (0–10, 10–30, and 30–100 cm) (Fig. 2b). The vertical discretization follows the established EcoPlot-iso configuration and effectively represents vertical gradients in soil moisture and isotopic composition, broadly consistent with soil moisture and isotope measurements within each layer. Recently, the isotope tracking module was further developed to include fractionation and mixing processes, allowing EcoPlot-iso to better constrain the partitioning between evaporation and transpiration and improve water flux estimates. The required input variables (Table 2) include meteorological data such as precipitation, potential evapotranspiration (PET), air temperature, and relative humidity, along with stable water isotopic data (precipitation isotope) and vegetation-related parameters (leaf area index, LAI).

In EcoPlot-iso, canopy surface cover fraction (SCF) is derived from LAI using Beer's law with an extinction coefficient rE (Eq. S1). Maximum canopy storage is determined by the SCF and an interception threshold parameter α . Interception is represented by a nonlinear saturation-type function (Eq. S2), whereby precipitation is first stored in the canopy until maximum canopy storage is reached, and any excess is routed as throughfall. Potential evapotranspiration PET is partitioned into canopy and soil fractions according to SCF (Eqs. S3 and S4). The canopy fraction drives evaporation from the interception store and transpiration from the soil layers, while the soil fraction drives evaporation from the

Table 1. Summary of observed soil types and soil moisture data at the three forest sites.

Site	Soil Type	Texture	Layer	Soil Moisture (mm)				Period
				Max	Min	Mean	SD	
Broadleaf forest	Brown earth	Loamy sand/sand	0 to 10 cm	26.3	3.5	13.7	6.3	2018.6–2024.12
			10 to 30 cm	56.2	6.9	24.7	11.7	
			30 to 100 cm	147.5	25.8	71.7	33.5	
Conifer forest	Sandy brown earth	Coarse sand	0 to 10 cm	28.7	8.6	17.3	7.1	2019.3–2024.12
			10 to 30 cm	53.8	2.6	21.8	12.3	
			30 to 100 cm	34.7	2.7	15.9	8.0	
Agroforestry	Podsollic brown earth	Loamy sand/sand	0 to 10 cm	32.1	10.4	21.3	7.8	2019.3–2024.12
			10 to 30 cm	53.4	7.2	29.8	13.5	
			30 to 100 cm	223.6	86.8	163.4	42.0	

upper soil layer (Eqs. S5–6). Actual fluxes are constrained by water availability: interception evaporation depends on canopy storage, transpiration is sequentially satisfied from the upper to deeper soil layers according to the relative soil-moisture availability (STO/S_{max}) of each layer (Eqs. S7–9), and soil evaporation is limited by moisture availability in the upper soil. Surface runoff is represented using a Hortonian threshold approach, where precipitation in excess of infiltration capacity is routed as runoff (Eq. S10). Preferential flow is triggered when throughfall exceeds a threshold, with a calibrated parameter controlling the bypass proportion (Eq. S11). Percolation, compartment flow and groundwater recharge are represented as storage–discharge relationships, where outflows are parameterised as power functions of soil or groundwater storage (Eqs. S12–14). Groundwater recharge is defined as the downward percolation flux at the lower boundary of the soil domain (30–100 cm layer), corresponding to a total soil depth of 1 m. Full variable definitions and governing equations are provided in Table S1 of the Supplementary Material (Eqs. S1–14).

EcoPlot-iso has been applied in diverse climatic and hydrological settings, including a one-year simulation in Scotland (Stevenson et al., 2023), a one-year simulation at the Demnitzer Millcreek (DMC) site in the Northern European Plain (Landgraf et al., 2023), and a four-year simulation in the humid tropics of Costa Rica (Birkel et al., 2024). Building on these applications, this study employs EcoPlot-iso for a long-term tracer-aided ecohydrological simulation to assess the effects of different forest management scenarios on water partitioning and ecohydrological resilience.

3.2 Model Adaptations: Integrating Root Distribution into the Transpiration Equation

Although root water uptake plays a critical role in soil–plant–atmosphere interactions, the vertical rooting distribution and the associated depth-dependent uptake efficiency were not explicitly represented in EcoPlot-iso (Stevenson et al., 2023). The current study introduces a novel depth-dependent root

uptake function to improve the model’s simulation of transpiration and water partitioning across different root distributions. This adaptation enables the model to account for variations in rooting depth and water uptake efficiency across land use types – such as young and mature forests or contrasting vegetation covers – that affect soil water extraction. Specifically, a new transpiration equation was implemented to calculate root water uptake across three soil compartments – upper, middle, and deep – by incorporating depth-specific uptake efficiency:

$$T_{p1} = r_{L1} \cdot (T_P - E_i) \cdot \left(\frac{S_U}{S_{U,max}} \right) \quad (1)$$

$$T_{p2} = r_{L2} \cdot (T_P - E_i - T_{p1}) \cdot \left(\frac{S_M}{S_{M,max}} \right) \quad (2)$$

$$T_{p3} = r_{L3} \cdot (T_P - E_i - T_{p1} - T_{p2}) \cdot \left(\frac{S_D}{S_{D,max}} \right) \quad (3)$$

where T_{p1} , T_{p2} , T_{p3} represent the transpiration from the upper, middle, and deep soil compartments, respectively. T_P denotes the canopy fraction of potential evapotranspiration. E_i denotes the canopy evaporation. S_U , S_M , S_D represent the water storage in the upper, middle, and deep soil compartments. $S_{U,max}$, $S_{M,max}$, $S_{D,max}$ are the maximum water storage capacities of these compartments. r_{L1} , r_{L2} and r_{L3} represent the root water withdrawal efficiency in the upper, middle, and deep soil compartments, respectively.

To explicitly link root water uptake to soil moisture availability and transpiration demand, an efficiency factor $r(z)$ was introduced. The exponential root water withdrawal efficiency function is defined as:

$$r(z) = e^{-\beta z} \quad (4)$$

where $r(z)$ represents the capacity of roots to extract water at depth z , and β is the decay rate (m^{-1}), which determines how quickly root activity decreases with increasing depth. A higher β value concentrates root activity near the surface, while lower β values allow for deeper water uptake (see

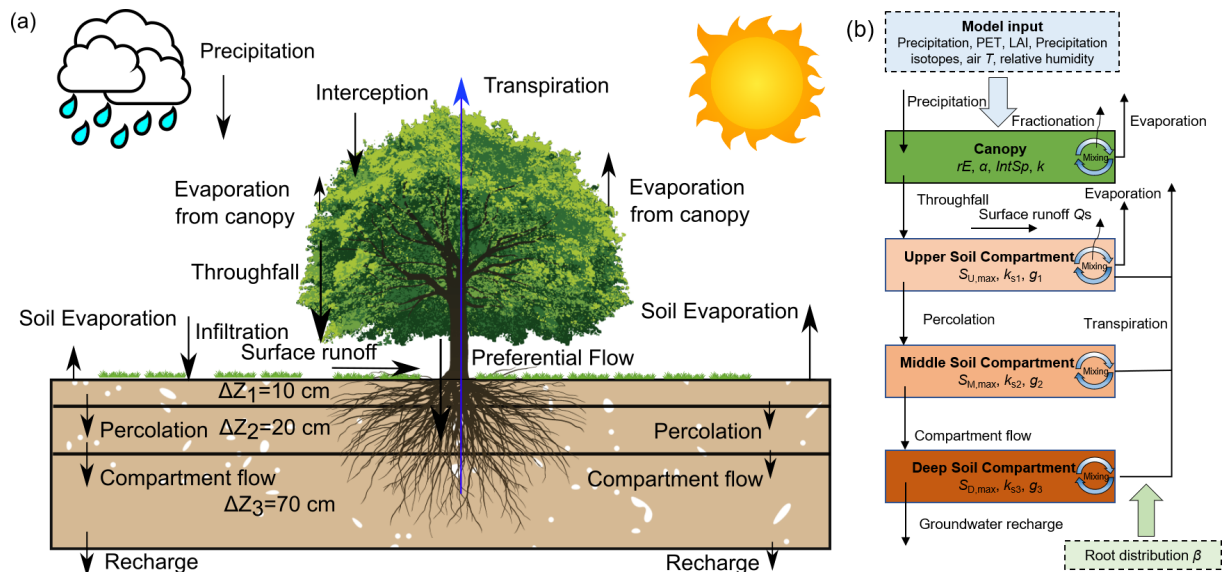


Figure 2. (a) Schematic representation of the ecohydrological fluxes and water partitioning in the EcoPlot-iso model illustrating major water fluxes and storage components; (b) conceptual framework and key parameters of the EcoPlot-iso model (Landgraf et al., 2023; Stevenson et al., 2023), highlighting the key ecohydrological processes simulated in this study.

Fig. S2 in Supplement). This formulation builds on the common assumption that potential root water uptake decreases exponentially with depth (Li et al., 1999; Wu et al., 1999) and is intentionally simplified for a plot-scale, data-constrained model setup. The soil profile is discretized into three layers (0–10, 10–30, and 30–100 cm; Fig. 2a), and r_{L1} , r_{L2} , and r_{L3} are calculated by evaluating $r(z)$ at the midpoint depth of each layer ($z = 5, 20,$ and 65 cm, respectively). These layer-specific efficiency values are then used as weighting coefficients in Eqs. (1)–(3) to calculate transpiration from each of the three soil compartments.

3.3 Model Setup, Input and Observation Data

The EcoPlot-iso model was applied to DMC across five sites with different dominant land use: broadleaf forest, conifer forest, agroforestry, cropland and grassland over a 25-year period (2000–2024) at daily timesteps. Soil moisture initialization was based on observed data, and a one-year spin-up period was included before each simulation to stabilize initial conditions. The input datasets required for the model – climate, vegetation, soil moisture, and stable water isotope data – are summarized in Table 2. Climate variables, including precipitation, temperature, wind speed, and relative humidity, were primarily obtained from the Müncheberg weather station (DWD, German Weather Service, ~ 20 km from DMC). Potential Evapotranspiration (PET) was calculated using the FAO Penman-Monteith equation, while net radiation was derived from ERA5 reanalysis data (Hersbach et al., 2020). The Leaf Area Index (LAI) time series was extracted from the MODIS 8 d LAI product at the location of each study site and linearly interpolated to daily

timesteps. To improve accuracy and reduce data noise, the MODIS LAI was further bias-corrected against in-situ LAI measurements (maximum and minimum values), following Smith et al. (2021) and Wu et al. (2023). Given the plot-scale setup of EcoPlot-iso, agroforestry systems, characterized by mixed crop–tree vegetation, are represented implicitly using MODIS-derived LAI and calibration against plot-scale soil moisture and isotope observations, rather than explicitly resolving multiple vegetation types. In addition, the complete set of time series input data used to drive the EcoPlot-iso simulations in the Demnitzer MillCreek Catchment for 2000–2024 – including daily precipitation, precipitation isotopes ($\delta^2\text{H}$), air temperature, relative humidity, Leaf Area Index (LAI), and potential evapotranspiration (PET) – is presented in Figure S3 of the Supplementary Material.

Surface soil moisture (0–10 cm) was measured using a handheld soil moisture device (Theta handheld probe ML3 Sensor) on a monthly basis during two field observation periods (2018–2019 and 2021). For subsurface soil moisture, permanently installed probes were used: SMT-100 at forest and grassland sites, and CS650 at agroforestry and cropland sites. Measurements were recorded at 15-minute intervals with two replicates per depth. To facilitate data processing and consistency, all soil moisture datasets were aggregated into daily mean values, resulting in one volumetric water content value per site and soil depth. Details of the measurement devices, depth intervals, and aggregation methods are summarized in Table S2. Daily precipitation samples for stable water isotope analysis from June 2018 onward were collected at the Hasenfelde AWS, and earlier data were obtained from the Berlin weather station. Soil water isotopes were

sampled from bulk soil at the four plot sites at five depths (0–5, 5–10, 10–20, 20–30, and 30–50 cm) every 3–4 weeks during the growing season. The isotope data were aggregated according to the thickness of the corresponding model soil compartments. All isotope values are reported relative to Vienna Standard Mean Ocean Water (VSMOW). Further details on site instrumentation and data collection are described in Landgraf et al. (2022).

3.4 Model Calibration and Validation

The EcoPlot-iso model was calibrated using the Monte Carlo approach combined with a multi-criteria evaluation based on soil moisture and soil water isotope observations at each land use site. For each calibration, 100 000 parameter sets were generated using the Latin Hypercube Sampling (LHS) within a Monte Carlo framework (McKay et al., 1979) to broadly sample the parameter space and capture a wide range of plausible model behaviors.

The initial parameter ranges were defined based on literature values and site-specific knowledge. Specifically, initial ranges for the radiation extinction factor (rE) were guided by vegetation-specific light attenuation coefficients from canopy gap-fraction theory (Larcher, 1975; Gigante et al., 2009), using typical reference values of 0.35 for grasslands, 0.45 for croplands, and 0.65 for forests. Initial ranges for the interception storage capacity parameter (α) were guided by scaling values reported in global syntheses of canopy interception storage (Zhong et al., 2022) and interception sensitivity studies (Davies-Barnard et al., 2014), accounting for differences in model time step and formulation. The resulting interception evaporation is consistent with observational studies indicating that canopy interception losses typically represent approximately 10 %–30 % of annual precipitation in forested systems (Staelens et al., 2008; Llorens and Domingo, 2007).

Model performance was evaluated using the modified Kling-Gupta Efficiency (mKGE) (Kling et al., 2012), calculated separately for soil moisture (mKGE_{sm}) and soil water isotopes (mKGE_{iso}) at each of the three soil depth layers. Calibration followed a two-step refinement process. In the first step, based on the initial parameter ranges, parameter sets were retained only if they fell within the intersection of the top 60th percentile of all six individual mKGE metrics (i.e. soil moisture and soil water isotopes at each of the three soil depths). This step substantially reduced the number of parameter sets from the initial 100 000 samples. This intersection-based filtering ensured that retained simulations performed consistently well across all evaluated variables and depths. By retaining only the performance metrics and corresponding parameter sets, this step efficiently screened the parameter sets while substantially reducing data storage requirements during the initial exploration.

In the second step, the model was re-run using the retained parameter sets obtained from Step 1. For these re-run simulations, an average *mKGE* value across depths and

variables was then used as the objective performance metric (Eq. 5), and the 100 best-performing simulations were selected for final analysis. The model parameters, their initial ranges, and the refined ranges for each of land use are summarized in Table S3 in the Supplement. To assess parameter constraints and equifinality, the probability density distributions and median values of the calibrated parameters were derived from the 100 best-performing simulations for each site (see Fig. S4). These were then used to evaluate the convergence of the parameters relative to their initial ranges.

$$mKGE = \frac{\sum_i^3 mKGE_{sm} + \sum_i^3 mKGE_{iso}}{6} \quad (5)$$

Model parameters were calibrated using the full available observation, comprising seven years of soil moisture data and three years of soil water isotope data, in order to maximise information content under limited isotope availability (Shen et al., 2022). To additionally assess model robustness beyond a shorter calibration window, a split-sample calibration–validation experiment was conducted consistently across all land-use types. In this experiment, the model was calibrated using an earlier subset of the soil moisture and isotope observations, followed by validation against an independent soil moisture period, as isotope observations were not available for validation. Results from this split-sample evaluation, which showed good parameter transferability across most sites, are reported in Table S4 and Figs. S5–7 of the Supplement. Given this transferability, the full-period calibration was retained for the main scenario simulations, as it provides more stable parameter estimates under data limitations, while the split-sample results are presented for transparency and robustness assessment.

3.5 Development and Application of a Generic Forest Management Scenario Framework

The primary goal of this study was to develop a new, parsimonious and generic forest management scenario framework to evaluate how forest type, forest density, and root distribution – associated with forest age – influence long-term water partitioning and ecohydrological resilience under comparable environmental conditions. This framework was designed to capture the dominant effects of vegetation structure – such as interception and transpiration through canopy and root networks – on water partitioning, rather than to reproduce detailed species-specific physiology.

Based on this conceptual framework, baseline simulations covering the period 2000–2024 were established using EcoPlot-iso model at three forest sites within the DMC (broadleaf forest, conifer forest, and agroforestry). These baseline simulations provide forest-type-specific reference conditions against which alternative management scenarios were evaluated.

To isolate the effects of forest management from site-specific soil properties and boundary conditions, we ex-

Table 2. Summary of the used climate, vegetation, soil moisture, and isotope data.

Data	Unit	Period	Timestep	Acquisition
Climate data				
Precipitation	mm d ⁻¹	2000–2024	Daily	Muencheberg weather station (52.52°, 14.12°)
Temperature	°C			
Windspeed	m s ⁻¹			
Relative humidity	%			
Net shortwave radiation	W m ⁻²		Hourly	ERA5
Net longwave radiation				
Potential evapotranspiration	mm d ⁻¹		Daily	FAO Penman-Monteith equation
Vegetation data				
Leaf area index	–	2000–2024	8 d	MODIS at broadleaf forest, coniferous, and agroforestry sites
Soil data				
Soil moisture	%	2018–2024	Daily	broadleaf forest, cropland, agroforestry, and grassland sites
Isotope data				
Precipitation isotope $\delta^2\text{H}$	‰	2000–2024	Daily	Hasenfelde (52.41° N, 14.19° E), weather station in Berlin
Soil water isotope		2018–2019, 2021	Daily	Manually at broadleaf forest, cropland, agroforestry, and grassland sites

tended the observed forest-site configurations by systematically combining forest-type-specific vegetation parameter sets with site-specific soil parameter sets, derived from the corresponding baseline calibrations, resulting in a 3×3 scenario matrix (Fig. 3). The diagonal entries represent the observed site-based reference configurations – namely, Broadleaf forest site, Conifer forest site, and Agroforestry site – and are therefore treated as baseline scenarios. The remaining cross-combinations represent hypothetical but plausible forest-site (soil) configurations, in which vegetation characteristics are applied to alternative site-specific soil hydraulic properties and boundary conditions (e.g., soil texture and compaction). This design enables vegetation effects to be assessed independently of site-specific controls for scenario analysis, while acknowledging that vegetation and soil controls may not be fully independent and that soil hydraulic properties and boundary conditions remain inherently site-dependent. Ensemble-based comparisons across site configurations for each forest type therefore support a more robust and generic interpretation of ecohydrological behaviour.

Specifically, for each of forest-site baseline scenario calibration, we retained the top 100 best-performing simulations – ranked by average mKGE – and their corresponding parameter sets (as described in Sect. 3.4). Forest-type-specific vegetation parameters (rE , α) were derived from site-specific calibrations for broadleaf, conifer, and agroforestry systems,

and their median values from the 100 best-performing simulations at each site were used to represent characteristic vegetation conditions. The root distribution parameter (β) was not treated as strictly vegetation-specific, but as jointly influenced by vegetation type, soil properties, and soil water availability (Fig. S4). This ensemble-based selection was used to reduce parameter uncertainty and equifinality effects. These calibrated parameter sets were then used for subsequent scenario simulations to ensure physically consistent parameter configurations across all forest types. In contrast, soil-related parameters (k_{s1} , k_{s2} , k_{s3} , $S_{U,max}$, $S_{M,max}$, $S_{D,max}$, I_c , g_1 , g_2 , g_3 , PF_{scale}) were retained from the corresponding forest sites to preserve site-specific hydraulic properties and boundary conditions.

For vegetation forcing, we used forest-type-specific observed LAI time series (broadleaf, coniferous, and agroforestry), derived from the MODIS LAI products, described in Sect. 3.3 (Table 2; Fig. S3d). Forest-type-specific initial soil moisture conditions for the three soil layers were kept consistent with the corresponding baseline simulations. All scenario simulations were driven using identical climate input data, precipitation isotope time series, and potential evapotranspiration forcing as the baseline simulations to isolate the effects of forest characteristics and management.

The scenario framework varied three key dimensions of forest management:

- a. Forest type was varied by implementing three canopy types – broadleaf, conifer, and agroforestry – each assigned type-specific vegetation parameters and LAI time series to reflect differences in canopy structure.
- b. Forest density was varied by multiplying the reference LAI by a scaling factor ranging from 0.2 to 1.8. Higher forest density was represented by scaling factors > 1.0 , indicating denser canopy cover, while lower forest density corresponded to factors < 1.0 , reflecting more open canopy conditions. The applied LAI scaling range (0.2–1.8) follows previous tracer-aided modelling approaches (Neill et al., 2021) and spans realistic management-induced variability in canopy density, while remaining consistent with reported LAI values for mature European forests (Leuschner et al., 2006).
- c. Root water uptake efficiency was varied by scaling the site-calibrated β parameter to represent contrasting vertical root distributions associated with forest developmental stage. Three rooting scenarios were considered: $0.5 \times \beta$, $1.0 \times \beta$, and $2.0 \times \beta$, where β is the calibrated value for each forest site. Lower scaled values ($0.5 \times \beta$) represent more developed forests with deeper, less surface-weighted rooting systems, while higher scaled values ($2.0 \times \beta$) represent younger or less-developed forests with shallower, more surface-weighted rooting distributions (see Fig. S1). The $1.0 \times \beta$ scenario corresponds to the observed rooting distribution at each forest site.

Within this framework, LAI and rooting distribution were treated as independent scenario dimensions. LAI scaling represented management-induced changes in canopy density, whereas rooting distribution scenarios reflected contrasts in belowground water uptake. Their combined effects on water fluxes were evaluated without assuming a fixed linkage between canopy structure and rooting depth. This separation acknowledges that canopy density can change rapidly through management (e.g., thinning or harvesting), while rooting characteristics typically reflect longer-term stand development, thereby allowing realistic representation of above- and belowground controls on water partitioning.

Although EcoPlot-iso was originally developed for plot-scale applications, it is applied here to represent ecohydrological fluxes in a range of well-characterized sites within the DMC region. The model employs a one-dimensional approach that does not explicitly account for lateral fluxes; however, this simplification is intentional. It enables clearer interpretation of process-level dynamics under contrasting vegetation and climate conditions, making it suitable for general scenario analysis. This assumption is especially justified in the DMC catchment, which is characterized by flat, lowland topography and is predominantly governed by vertical hydrological fluxes (Kleine et al., 2021; Smith et al., 2020).

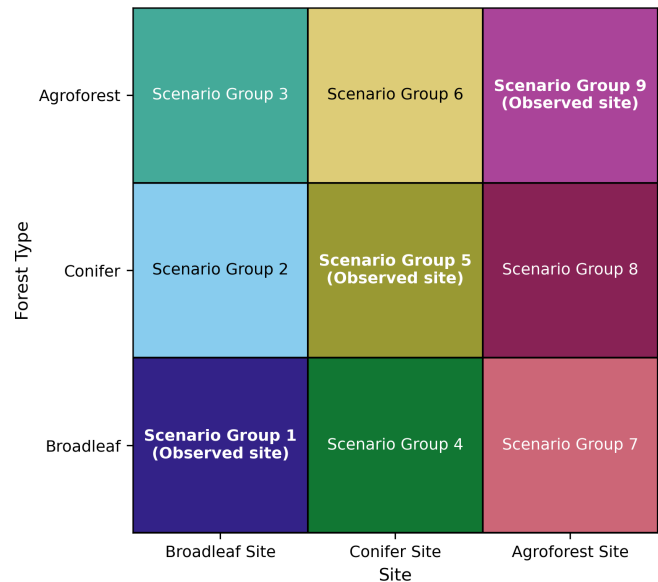


Figure 3. Matrix of nine Scenario Groups formed by combining three site-specific configurations (Broadleaf Site, Conifer Site, and Agroforest Site) with three forest types (Broadleaf, Conifer, and Agroforest). Each colored block represents a Scenario Group consisting of multiple sub-scenarios (e.g., varying forest densities and root water uptake distributions). Diagonal entries (Scenario Groups 1, 5, and 9), marked as “observed configuration”, correspond to forest–site combinations observed at the field sites, where vegetation type and site-specific soil–hydraulic and boundary conditions are consistent with real-world conditions.

The framework is not intended to reproduce exact spatial patterns or detailed species-specific physiology, but rather to capture the dominant effects of vegetation structure on vertical water fluxes and soil moisture dynamics. By focusing on variations in forest type, forest density, and root distribution associated with forest age and management, the framework enables a generalized assessment of long-term water partitioning and ecohydrological resilience under comparable environmental conditions. As such, it provides a practical and transferable tool for evaluating forest management impacts on water availability and ecohydrological resilience in drought-sensitive lowland catchments.

4 Results

4.1 Dynamics of Soil Moisture and Soil Water Isotopes at the Broadleaf Forest Site

Figure 4 shows the 25-year baseline simulations of soil moisture and soil water isotopes dynamics at the broadleaf forest site at a daily time step as an example. In general, the model effectively captures the magnitude, variability, extremes, and timing of soil moisture dynamics. Surface soil moisture shows higher variability than deeper layers. Based

on the modified Kling-Gupta Efficiency (mKGE), soil moisture simulations generally perform better in the deep layer than in the upper and middle layers, though this may partly reflect the more limited variance in deeper soil moisture. In addition, the model slightly overestimates low soil moisture in the deeper layers during wet summers (e.g., 2023, 2024) and underestimates soil moisture during dry winters (e.g., 2021 and 2022). Soil water isotope simulations also perform well, with higher mKGE values in the middle layer than in upper and deep layers. The uncertainty range of soil water isotope simulations is narrower than that of soil moisture, indicating lower uncertainty in the isotope predictions.

Table 3 shows the modified Kling-Gupta Efficiency (mKGE) and Root Mean Square Error (RMSE) values for soil moisture and soil water isotopes across different land use plots. In all other cases the mKGEs for soil moisture are similar to the broadleaved plot, and soil water isotopes are reasonably reproduced, indicating the model's robustness and transferability. These results provide strong support for the appropriateness of applying EcoPlot-iso to assess the impacts of alternative forest management scenarios in subsequent analyses. In addition, simulated evapotranspiration was independently evaluated against MODIS-derived ET for all land use types, with model performance quantified using RMSE and mKGE metrics (Table S4). This independent evaluation provides further support for the model's ability to reproduce key water fluxes beyond the variables used for calibration.

4.2 Water Balance Components Under Different Wetness Conditions at the Broadleaf Forest Site

Figure 5 presents the mean monthly water balance components and their changes between dry and wet years for the baseline simulation at the broadleaved forest site from 2000–2024. Groundwater recharge dominates blue water fluxes, while surface runoff is rare and occurs only during extreme summer rainfall events (Fig. 5a). Transpiration and canopy evaporation dominate in summer, while soil evaporation peaks in spring. Across dry and wet years, groundwater recharge shows the strongest sensitivity to interannual wetness, with reduced recharge during dry years and enhanced recharge during wet years following precipitation anomalies (Figs. 5b and S1). In contrast, transpiration remains relatively stable despite differences in annual wetness, indicating resilient vegetation function. This stability likely reflects the mature age of the forest (~ 60 years), although gradual changes in forest structure over the 20-year period may also play a role. Corresponding water balance results for the conifer forest and agroforestry sites are provided in the Supplementary Material (Fig. S9). Across the three forest types, the conifer forest exhibits the largest changes in groundwater recharge between dry and wet years, particularly in August, whereas agroforestry shows comparatively smaller changes than the broadleaf forest, indicating higher ecohydrological resilience. Overall, these seasonal patterns offer key insights

into water partitioning under three forest baseline conditions and establish an important baseline for evaluating the impacts of alternative forest management scenarios.

4.3 Impacts of Forest Management on Water Partitioning and Soil Moisture

Results in this section are based on the full forest management scenario framework, including all nine forest-site Scenario Groups and their associated ensemble simulations (Fig. 3), rather than on the observed baseline configurations alone.

4.3.1 Water Balance and Partitioning Across Forest Types

Figure 6 compares the mean annual water balance components across broadleaf forest, coniferous forest, and agroforestry types based on the ensemble mean of simulations derived from the paired vegetation-site soil parameter configurations (Fig. 3), under reference canopy and rooting conditions (LAI scaling = 1; $\beta = 1 \times \beta$). Results showed that evapotranspiration under coniferous forests accounted for 7 % more of annual precipitation than broadleaf forest, and 11 % more than in agroforestry systems. This was primarily due to higher transpiration (T_r) and canopy interception evaporation (E_i). Accordingly, soil evaporation (E_s) and groundwater recharge (Recharge) were lowest in conifers and highest in agroforestry. Agroforestry had 11 % more groundwater recharge relative to annual precipitation than conifers, and 4 % more than broadleaf forests. Across forest types, the largest fraction of transpiration originated from the upper soil layer (T_{r_upper}), reflecting its closer coupling to precipitation inputs and higher soil moisture availability, while surface runoff (Q_s) remained minimal and nearly identical. These results reflect the influence of forest structure and canopy cover on ecohydrological partitioning, with coniferous systems favoring atmospheric losses and agroforestry promoting soil evaporation and subsurface recharge. They underscore the trade-offs between evapotranspiration and groundwater recharge across different forest types.

Figure 7 presents ternary diagrams illustrating the relative partitioning of key water flux components across three forest types based on individual simulations from the paired vegetation-site soil parameter configurations under reference canopy and rooting conditions. Transpiration predominates in all three forest types (Fig. 7a). The conifer forest exhibits a distinct pattern, characterized by the lowest soil evaporation (E_s) and the highest interception evaporation (E_i) partitioning compared to broadleaf forest and agroforestry systems (Fig. 7a). In terms of green-blue water partitioning, the agroforestry system shows the largest groundwater recharge contribution (Fig. 7b). Figure 7b also highlights a clear trade-off between transpiration and groundwater recharge, reflecting both equifinality among the 100 best-

Table 3. Model performance metrics for soil moisture and soil water isotopes ($\delta^2\text{H}$) at each land use site over the full evaluation period (2000–2024), evaluated using the modified Kling–Gupta Efficiency (mKGE) and the root mean square error (RMSE, mm for soil moisture and ‰ for $\delta^2\text{H}$). Metrics are computed by comparing observed and simulated time series at each soil depth.

Sites	Soil moisture						Soil water isotope ($\delta^2\text{H}$)					
	Upper		Middle		Deep		Upper		Middle		Deep	
	mKGE	RMSE	mKGE	RMSE	mKGE	RMSE	mKGE	RMSE	mKGE	RMSE	mKGE	RMSE
Broadleaf Forest	0.56	5.83	0.75	7.51	0.84	13.32	0.58	13.23	0.74	8.35	0.68	8.43
Conifer forest	0.61	5.77	0.68	8.68	0.70	5.56	0.67	11.69	0.80	6.94	0.50	13.09
Agroforestry	0.72	5.22	0.79	6.63	0.77	23.43	0.82	8.09	0.85	10.45	0.79	8.98
Grassland	0.89	1.67	0.71	6.18	0.72	16.01	0.71	9.07	0.77	7.69	0.61	8.36
Cropland	0.53	5.84	0.62	8.88	0.71	22.36	0.83	8.36	0.85	9.19	0.36	13.71

performing parameter sets and differences in site-specific soil properties. Broadleaf and agroforestry forests display largely overlapping partitioning patterns overall, although interception evaporation and total evaporation differ notably between the two (Fig. 7a–b). Differences in soil properties also influence transpiration partitioning, following the order agroforestry site > broadleaf site > conifer site. The conifer site is characterized by coarse sandy soil with lower water retention and faster drainage, whereas the agroforestry site has greater water-holding capacity, which likely contributes to the observed differences in transpiration.

4.3.2 Annual Mean Water Flux Responses to Forest Management Scenarios

The annual mean responses of key ecohydrological fluxes to forest management scenarios across all paired vegetation–site configurations are summarized in Fig. 8, while the detailed number and visualization of green and blue water partitioning are provided in the Fig. S10 in Supplement. Figure S10 presents heatmaps of evapotranspiration (ET), groundwater recharge (Recharge), transpiration (Tr), ET partitioning (ET/P), groundwater recharge partitioning (Recharge/P) and green water partitioning (Tr/ET) for agroforests, broadleaf forest, and coniferous forest scenarios.

Across all forest management scenarios, annual mean evapotranspiration ranges from 285 to 454 mm yr⁻¹, with ET fraction relative to precipitation varying between 0.52 and 0.84 (Fig. S10). In contrast, groundwater recharge ranges from 85 to 254 mm yr⁻¹, reflecting strong sensitivity to vegetation structure and canopy density. Annual mean transpiration (Tr) varies between 77 and 261 mm yr⁻¹, with the corresponding green water partitioning (Tr/ET) ranging from 0.27 to 0.64. These results underscore the significant influence of vegetation type and structure on ecohydrological fluxes and water partitioning outcomes.

Consistent with these detailed patterns, Fig. 8 shows that both transpiration and evapotranspiration increase with higher LAI scaling factors, while groundwater recharge decreases. Figure 8a and b illustrate the trade-off between in-

creased ET and reduced groundwater recharge under different forest management scenarios. ET and transpiration rise rapidly at first, then slow down and transpiration even slightly decreases for conifer forests due to increased interception evaporation and soil moisture limitation (Fig. 8c and i). This decline is not observed in broadleaf or agroforestry systems, likely due to their different seasonal LAI patterns. While summer LAI values for broadleaf and coniferous forests may be similar, the consistently high year-round LAI in conifers can exacerbate moisture stress.

At higher LAI levels, transpiration decreases slightly while canopy interception evaporation increases (Fig. S11). In dense coniferous stands, excessive interception and persistently dry soils limit root water uptake, reducing vegetation function. This highlights a trade-off between transpiration and interception evaporation. The resulting moisture limitation suggests that such high-density forests may not be sustainable under water-limited conditions, as this negative feedback could constrain long-term forest growth and persistence. In addition, forests with shallow-rooted trees – such as young stands – tend to transpire less, generate more groundwater recharge, and exhibit lower Tr/ET ratios compared to deep-rooted forests. However, under high canopy density conditions, transpiration declines across rooting scenarios, suggesting that this reduction is driven not only by soil moisture limitation, but also by increased interception evaporation.

4.3.3 Monthly Dynamics of Water Fluxes Responses to Forest Management Scenarios

Figure 9 shows monthly deviations in water balance components across forest management scenarios, based on the ensemble mean of simulations derived from the paired vegetation–site soil parameter configurations (Fig. 3) under reference canopy and rooting conditions (LAI scaling = 1; $\beta = 1 \times \beta$). Relative differences among forest types indicate that agroforestry exhibits lower transpiration and canopy evaporation, but higher soil evaporation during summer compared to broadleaf forests (Fig. 9a). They are also associated

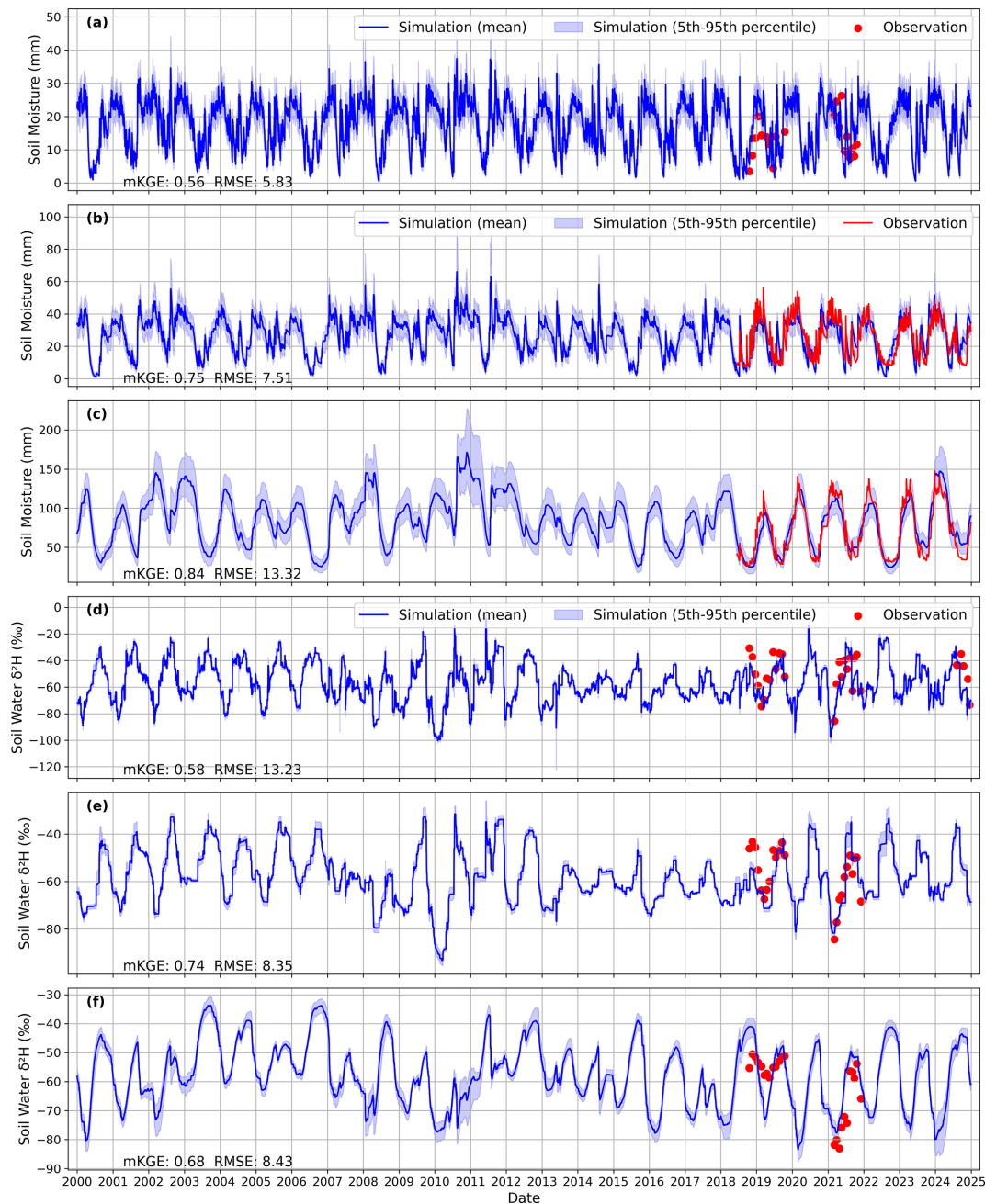


Figure 4. Long-term (2000–2024) simulations of soil moisture and soil water isotope ($\delta^{2}\text{H}$) at three different depths using EcoPlot-iso at a broadleaf forest site in the Demnitzer Millcreek catchment. (a–c) Simulated (mean \pm 5th–95th percentile) and observed soil moisture at upper (0–10 cm), middle (10–30 cm), and deep (30–100 cm) layers. (d–f) Simulated (mean \pm 5th–95th percentile) and observed soil water isotopic composition ($\delta^{2}\text{H}$) at corresponding depths. The blue line represents the mean value of the 100 best simulations, while the shaded area indicates the range between the 5th and 95th percentiles of these simulations. The red points and red line represent observed values. Modified Kling-Gupta Efficiency (mKGE) values for each simulation are indicated in the respective panels.

with greater groundwater recharge from summer through the following winter. A shift from broadleaf to conifer forests is expected to have a greater impact on the water balance than the shift from agroforest to broadleaf (Fig. 9a and b). Compared to broadleaf forests, conifer forests exhibit higher sim-

ulated transpiration in March (Fig. 9b), driven by increased potential evapotranspiration and a relatively higher leaf area index (LAI) under wet soil conditions. This difference diminishes as the LAI of broadleaf forests increases in spring.

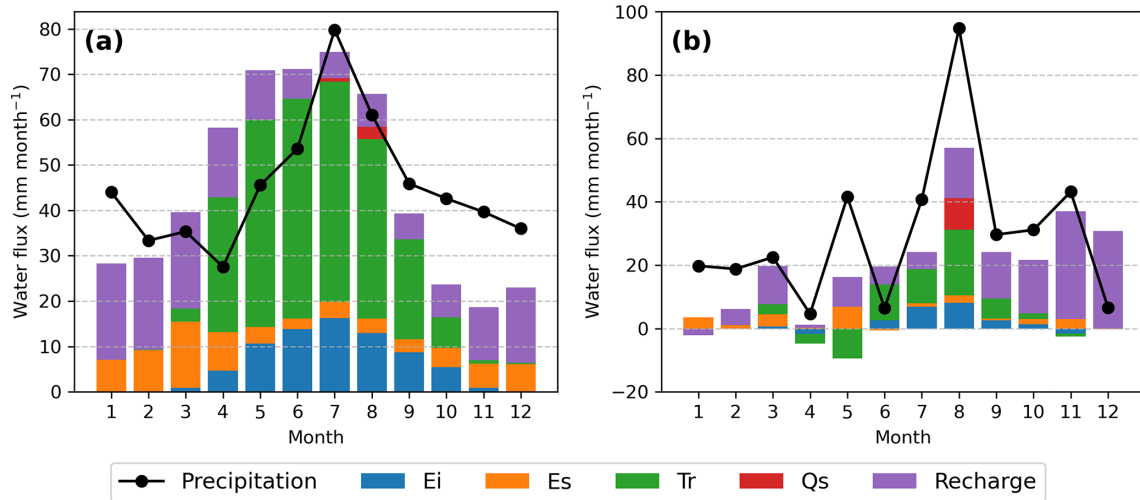


Figure 5. Mean monthly water balance components for the broadleaf forest site in the Demnitzer Millcreek catchment over 2000–2024, simulated with EcoPlot-iso using the mean of the best 100 parameter sets (see Sect. 3.4 for details). Stacked bars show monthly totals of interception evaporation (Ei), soil evaporation (Es), transpiration (Tr), surface runoff (Qs), and groundwater recharge, while the black line indicates precipitation (P). (a) Long-term mean monthly water balance (mm month⁻¹). (b) Differences between wet years (2002, 2007, 2010, 2023) and dry years (2006, 2018, 2022), expressed as wet minus dry (mm month⁻¹).

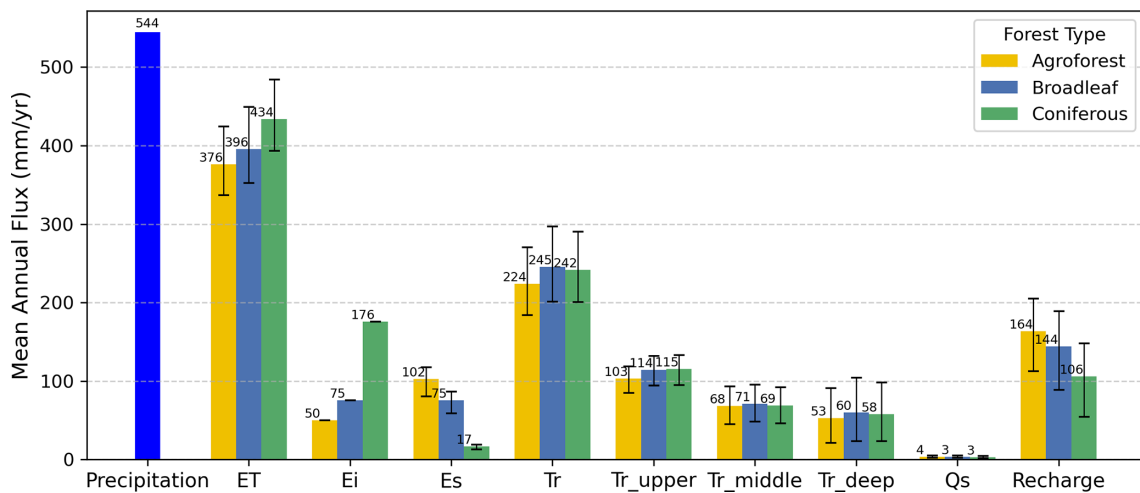


Figure 6. Comparison of mean annual water balance components across different forest types: broadleaf (blue), coniferous (green), and agroforestry (yellow). Bars represent the mean annual flux based on 25-year totals, with error bars indicating the 5th and 95th percentile ranges of the 100 best simulations. All simulations were conducted under baseline conditions with a fixed forest root parameter β of 0 and LAI scaling factor of 1.0.

Changes in the LAI scaling factor influence water balance components in summer, increasing transpiration and canopy evaporation while reducing recharge and soil evaporation (Fig. 9c and d). Increasing the LAI scaling factor from 0.4 to 1.0 has a greater impact than reducing it from 1.6 to 1.0, as vegetation water use responds more sensitively at low LAI values but plateaus at higher values due to energy or soil moisture limitations. Altering the forest root parameter (β), while using the same LAI time series, primarily affects deep-layer transpiration, reducing total transpiration and in-

creasing recharge. Other water balance components remain unchanged because the LAI time series is held constant.

Figure 10 extends the monthly analysis by explicitly comparing wet–dry-year differences in water balance responses across forest type, canopy density, and rooting scenarios. In contrast to Fig. 9, which presents mean monthly deviations relative to reference conditions, and Figure 5b, which shows the baseline wet–dry-year differences, Fig. 10 highlights how these wet–dry contrasts vary among scenarios, thereby isolating drought-sensitivity effects.

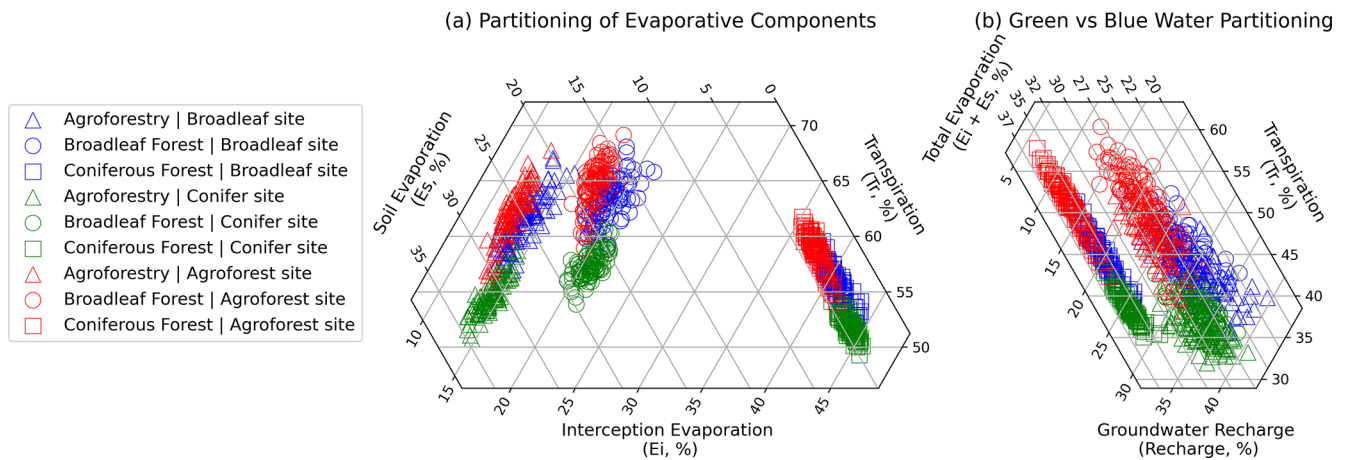


Figure 7. Water flux partitioning illustrated using ternary diagrams based on the 100 best model simulations derived from the paired vegetation–site soil parameter configurations for three forest types: agroforestry, broadleaf forest, and coniferous forest, under reference canopy and rooting conditions ($LAI_{scaling} = 1.0$; $\beta = 1 \times \beta$). (a) Partitioning of total evapotranspiration into transpiration (Tr), soil evaporation (Es), and interception evaporation (Ei). (b) Partitioning of water fluxes into green water (Tr and $E = Ei + Es$) and blue water (groundwater recharge). Each point represents the normalized annual mean flux from a 25-year simulation. Colored markers denote different forest types.

For agroforestry relative to broadleaf forests, hydroclimatic contrasts primarily affect groundwater recharge and transpiration, with the largest wet–dry differences occurring in late summer (Fig. 10a). This indicates a more buffered late-summer transpiration response in agroforestry systems under drought conditions. In contrast, differences between coniferous and broadleaf forests show the largest wet–dry contrasts in transpiration during May (Fig. 10b), rather than March as indicated by the mean monthly deviations in Fig. 9b. This seasonal shift indicates that conifer transpiration is most drought-sensitive during the later spring period, likely reflecting sustained year-round transpiration and associated soil moisture drawdown in conifer forests, and highlighting differences in early growing-season water-use strategies between coniferous and broadleaf forests. Figure 10c and d show that wet–dry differences are largest in summer (August), indicating that drought conditions amplify ecohydrological differences between low and high canopy density, as well as between shallow and deep rooting scenarios, particularly for transpiration and groundwater recharge. Overall, Fig. 10 demonstrates that hydroclimatic extremes not only modify the magnitude of vegetation controls on water partitioning but also shift their seasonal expression, with important implications for ecohydrological resilience under future drought conditions.

4.3.4 Soil Moisture Anomalies

Figure 11 shows the relative summer soil moisture anomalies across three forest types and three soil layers. Anomalies are calculated as the percentage deviation from the long-term seasonal mean, enabling normalized comparison across forest types and soil layers. Conifer forests exhibit the strongest

soil moisture anomalies, followed by broadleaf forests, while agroforests exhibit the least variability, indicating greater stability in soil moisture. Furthermore, among the three soil layers, the middle layer (10–30 cm) consistently shows stronger anomalies across all forest types, with magnitudes nearly double those of the other layers, highlighting its vulnerability during summer drought. In contrast, the upper layer (0–10 cm) and deep layer (30–100 cm) exhibit weaker anomalies, likely due to frequent soil moisture replenishment by summer rainfall in the upper layer and either more stable moisture retention or greater water storage capacity at depth that compensates for drought impacts. Negative soil moisture anomalies are more pronounced in summer than in spring, reflecting the stronger seasonal drought effects and fluctuations in soil moisture (see Fig. S12). During spring, broadleaf forests and agroforests display similar negative soil moisture anomalies, suggesting comparable seasonal soil moisture dynamics between these forest types.

5 Discussion

5.1 Vegetation Controls on Water Partitioning under Contrasting Forest Management Scenarios

Assessing the influence of different land use types on water availability is inherently challenging because of the complex interactions among vegetation, climate, and soil properties (te Wierik et al., 2021; Zhang et al., 2001). Different vegetation types have distinct water demands, and their contrasting canopy structures affect how precipitation is intercepted and partitioned into infiltration, runoff, groundwater recharge, and evapotranspiration (Brauman et

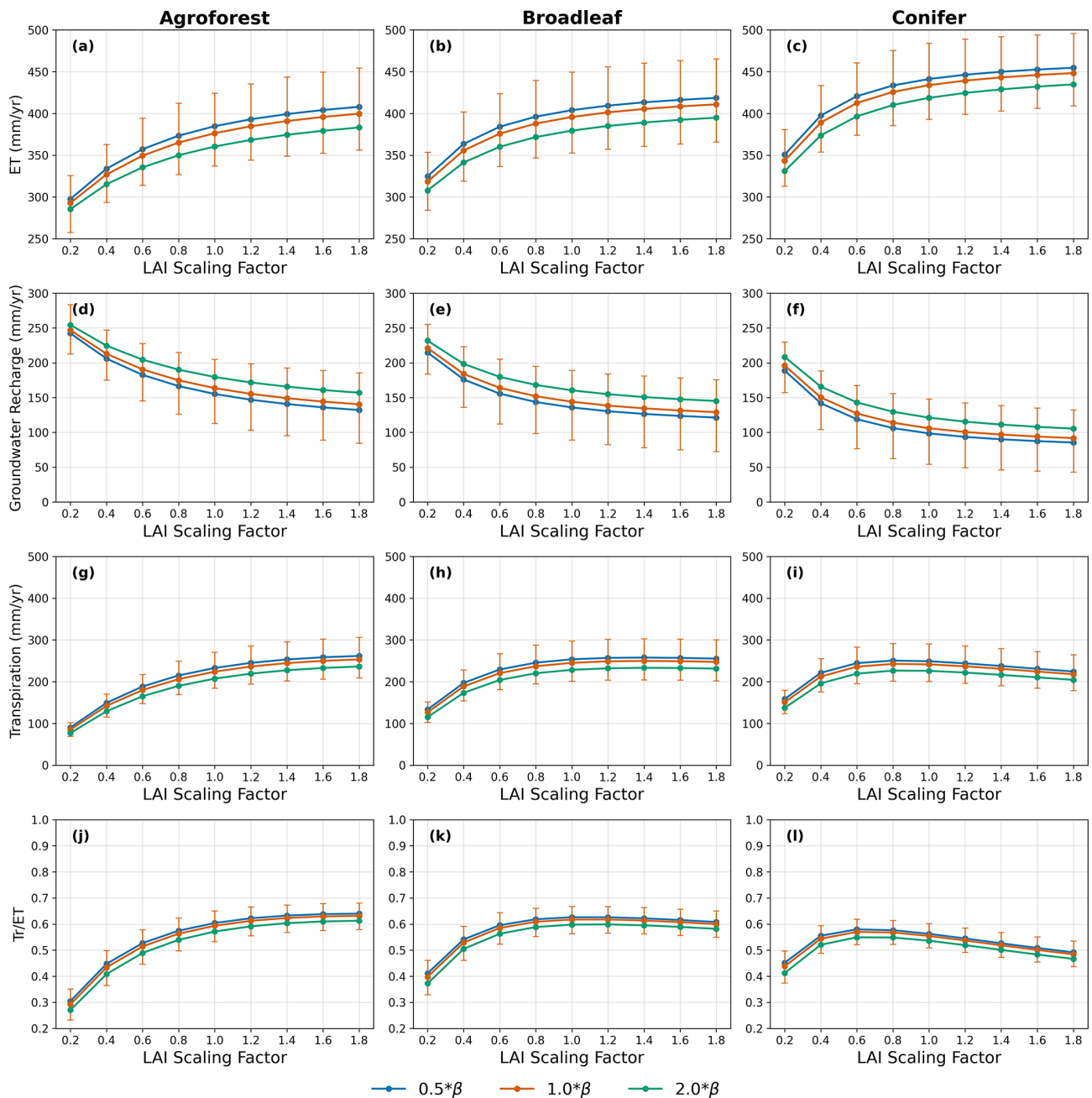


Figure 8. Annual mean ecohydrological fluxes for three forest types (Agroforest, Broadleaf, and Conifer) under varying LAI scaling factors and root depth scenarios, based on the ensemble mean of simulations derived from the paired vegetation–site soil parameter configurations (Fig. 3). Panels (a)–(c) show evapotranspiration (ET), (d)–(f) show groundwater recharge, (g)–(i) show transpiration, and (j)–(l) show the ratio of transpiration to total evapotranspiration (Tr/ET). Lines represent different rooting depth scenarios (β), while vertical bars denote the 5th–95th percentile range across ensemble simulations for the baseline rooting scenario ($\beta = 1 \times \beta$).

al., 2010). Vegetation management practices can substantially alter these processes. Moreover, the effects of vegetation and canopy structure may vary depending on underlying soil characteristics (Geris et al., 2015). This complexity poses a significant challenge for land managers and policymakers, particularly in drought-sensitive regions experi-

encing increasing aridity under climate change (Orth and Destouni, 2018). In such contexts, providing informed guidance on sustainable land cover choices is increasingly important for maintaining long-term water availability (Estrela and Vargas, 2012). In regions where forestry has traditionally been a dominant land use, shifting hydroclimatic conditions

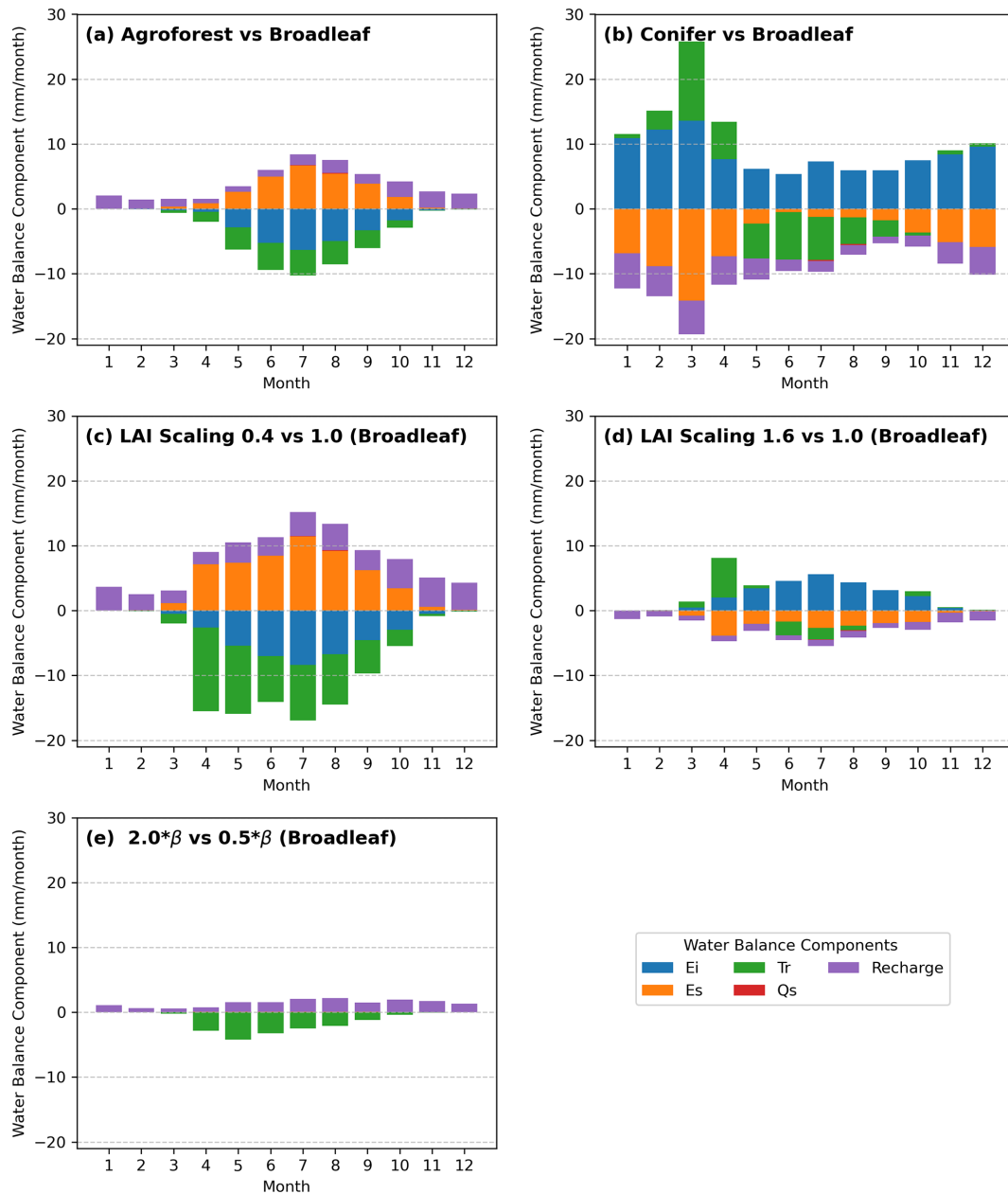


Figure 9. Monthly deviations of water balance components relative to the baseline broadleaf forest scenario, based on the ensemble mean of simulations derived from the paired vegetation–site soil parameter configurations (Fig. 3) under reference canopy and rooting conditions (LAI scaling = 1; $\beta = 1 \times \beta$). Each panel illustrates the deviation of monthly water balance components from the baseline simulation, with only one parameter modified in each scenario: **(a)** agroforest, **(b)** conifer forest, **(c)** LAI scaling factor = 0.4, **(d)** LAI scaling factor = 1.6, and **(e)** root parameter $\beta = 2.0$. Tr: transpiration, Ei: canopy evaporation, Es: soil evaporation, Qs: surface runoff, Recharge: groundwater recharge.

underscore the need to assess how different forest types and management practices affect water partitioning and drought vulnerability (Quandt et al., 2023). This requires evaluating water yield across multiple temporal scales, including the effects of forest management on annual and monthly water partitioning, and their implications for residual water availability – specifically streamflow generation and groundwater

recharge during low-flow periods (Brown et al., 2005; Neill et al., 2021).

Although complex, process-based ecohydrological models such as RHESSys and EcH₂O are well suited to capturing detailed interactions among hydrological processes and water fluxes in data-rich research settings, their broader application in forest and land management is often constrained by

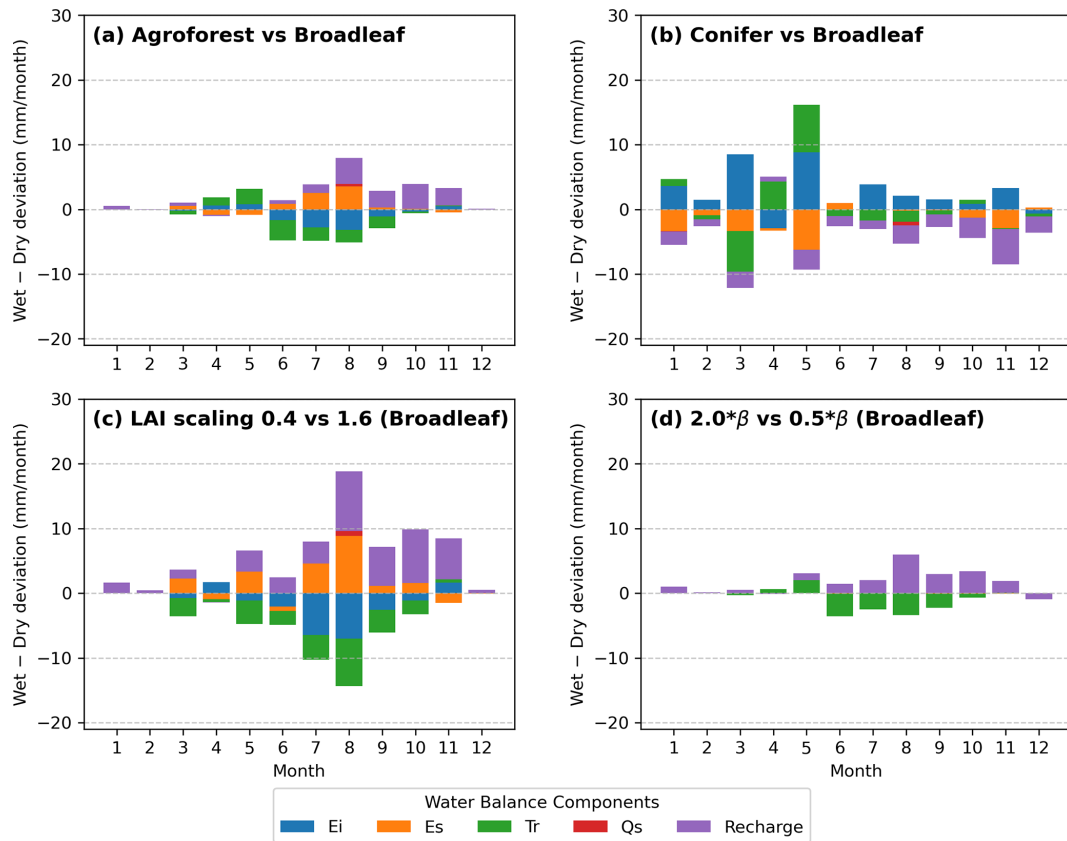


Figure 10. Monthly differences in water balance component deviations between wet and dry years across forest type, LAI scaling, and rooting (β) scenarios. For each panel, values show the difference between wet-year and dry-year deviations of a given scenario relative to its reference scenario; positive (negative) values indicate stronger (weaker) contributions during wet years. Panels show: **(a)** Agroforest vs. Broadleaf; **(b)** Conifer vs. Broadleaf; **(c)** LAI scaling 0.4 vs. 1.6 for Broadleaf; **(d)** $2.0 \times \beta$ vs. $0.5 \times \beta$ for Broadleaf. Stacked bars indicate contributions from interception evaporation (Ei), soil evaporation (Es), transpiration (Tr), surface runoff (Qs), and groundwater recharge (Recharge). Wet years are 2002, 2007, 2010, and 2023; dry years are 2006, 2018, and 2022.

the availability of observation data required for model forcing and calibration, as well as computational demand (Fatichi et al., 2012; Kuppel et al., 2018; Tague and Band, 2004). In this study, we therefore adopt a parsimonious, tracer-aided, conceptual process-based modelling approach. This was not to replace more complex models, but to provide robust and management-relevant insights into the dominant vegetation-structural controls governing water partitioning under different forest management scenarios. This focus is particularly relevant for Brandenburg, northeastern Germany, where recent droughts have highlighted the vulnerability of traditional forest management practices dominated by Scots pine plantations (Luo et al., 2024). By employing the tracer-aided ecohydrological model EcoPlot-iso, we developed and applied a generic framework to quantify the long-term effects of variations in forest type, forest density and root distribution on both blue and green water fluxes. The framework is based on idealized monoculture forest scenarios and explicitly acknowledges that additional species-specific and process-level dynamics (e.g., stomatal regulation, VPD sen-

sitivity, drought stress strategies) are not represented and remain important directions for future model development. While this study focused on idealized, homogeneous vegetation scenarios (broadleaf and conifer) for clarity and comparability, mixed crop–tree systems such as agroforestry could only be represented implicitly in EcoPlot-iso through aggregated plot-scale vegetation parameters. Species-specific interactions and sub-grid vegetation heterogeneity are therefore not explicitly resolved. The applied LAI scaling range represents an intentionally broad, management-relevant envelope for exploring canopy density effects, and scenario results should therefore be interpreted in a relative rather than prescriptive sense.

We acknowledge that the calibration of EcoPlot-iso is subject to parameter equifinality, whereby multiple parameter combinations can reproduce the observed soil moisture and isotope dynamics with similarly good performance. Rather than seeking a single optimal parameter set, our calibration strategy explicitly accounts for this equifinality by propagating uncertainty from the 100 best-performing simulations

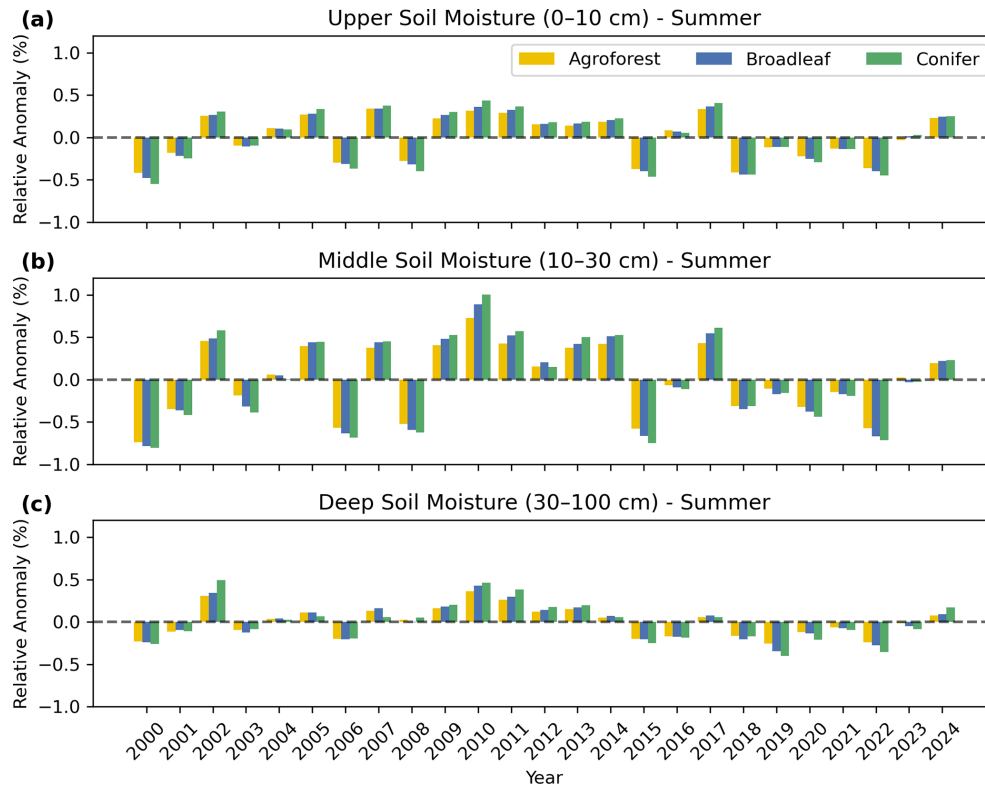


Figure 11. Relative summer (June–August) soil moisture anomalies across three soil layers: (a) upper (0–10 cm), (b) middle layer (10–30 cm), and (c) deep layer (30–100 cm) for three forest types (Agroforest, Broadleaf, Conifer). Results are based on the ensemble mean of simulations derived from the paired vegetation–site soil parameter configurations (Fig. 3) under reference canopy and rooting conditions (LAI scaling = 1; $\beta = 1 \times \beta$). Bars represent deviations from the long-term mean, with positive values indicating wetter conditions and negative values indicating drier conditions.

into all key results. The scenario framework further assumes that vegetation- and soil-related parameter sets can be recombined for comparative scenario analysis, without explicitly preserving parameter correlations among the calibrated ensembles. This may contribute to uncertainty inflation in some flux estimates and should therefore be considered when interpreting the prediction intervals. Uncertainty envelopes (5th–95th percentiles) shown in Figs. 4, 6, and 8 illustrate the range of annual and seasonal flux responses, enabling the magnitude of parametric uncertainty to be evaluated relative to differences among forest types and management scenarios. Although parametric uncertainty is non-negligible and in some cases comparable to different forest management scenarios, the main findings are supported by consistent ensemble-mean responses and clear directional differences in water partitioning across scenarios. Accordingly, results are interpreted in a relative and comparative sense, emphasizing management-relevant trade-offs rather than absolute flux predictions.

In the baseline simulations for broadleaf forest, conifer forest and agroforestry at the DMC site, the estimated mean annual evapotranspiration (ET) over 2000–2024 was 396, 434, and 376 mm yr⁻¹, respectively, accounting for approxi-

mately 73 %, 80 %, and 69 % of annual precipitation. These values are consistent with previous modelling studies at the DMC, which reported ET fractions ranging from 68 % to over 80 % of annual precipitation (Smith et al., 2021; Landgraf et al., 2023). Differences among studies may reflect interannual climate variability and the influence of particularly dry or wet years that are not captured by short-term assessments. Differences in model structure, parameterization, and input data may also contribute to the spread in reported ET values. In addition, to further assess model performance using an independent data source, simulated ET was evaluated against MODIS-derived ET for all land use sites in the DMC, including broadleaf forest, conifer forest, agroforestry, cropland, and grassland (Fig. S8 and Table S4). Model performance was quantified using mKGE metrics calculated from daily ET, providing an external validation independent of the calibration data. While EcoPlot-iso tends to slightly underestimate ET relative to MODIS observations, mKGE values indicate good agreement in temporal dynamics across land-use types, supporting the model’s ability to reproduce key ET variability. Overall, this evaluation underscores the importance of long-term simulations and independent data-based validation for capturing representative ecohydrological be-

havior and for assessing the impacts of forest management strategies under variable climatic conditions.

In catchments like DMC, where evapotranspiration (ET) is high, atmospheric demand is the primary driver of root water uptake, though vegetation plays a key role in regulating its impact on water availability. In Brandenburg, coniferous forests have traditionally been favored on sandy soils, but modelling indicates high water use due to interception losses and year-round transpiration potential (Fig. S9c). Consequently, the implications for both reduced groundwater recharge and reduced forest productivity have encouraged landowners to explore alternative land use, such as broadleaf forests and agroforestry. These options have the potential to optimize biomass productivity while enhancing landscape water retention, groundwater recharge, and drought adaptation.

These results (e.g., Figs. 8 and S10) have practical applications, such as estimating the direction and magnitude of the changes in evapotranspiration and water yield as a function of forest management practices, driven by alterations in canopy structure and rooting depth. The modelling approach thus provides useful insights into the hydrological implications of alternative canopy structures and rooting patterns for water use. Figure 12 compares the mean annual partitioning of water fluxes and soil moisture across broadleaf, coniferous, and agroforest types under dry and wet year conditions. It highlights how different vegetation strategies influence ecohydrological resilience, with substantial differences in water partitioning observed between dry and wet years across contrasting forest management scenarios. By simulating long-term water availability across alternating wet and dry years, EcoPlot-iso simulations suggest that agroforestry can support water availability in drought-sensitive catchments by sustaining groundwater recharge as the dominant blue-water flux.

5.2 Soil Moisture Dynamics and Root Water Uptake Processes across Forest Management Scenarios

At most of the monitoring plots in the DMC, groundwater is typically more than 3 meters below the ground surface (Ying et al., 2025). Therefore, except in older forest plots with deeply rooting trees, vegetation relies on soil moisture for root water uptake. Even for mature trees, there is evidence that most root water uptake occurs in the near-surface soil horizons, as demonstrated by Birkel et al. (2025), 20 km from the DMC. A global synthesis by Evaristo and McDonnell (2017) further supports this, indicating that $\sim 77\%$ of plant water uptake comes from shallow sources, with deeper groundwater use primarily in more arid regions. While hydraulic redistribution may provide deeper access for some species (Emerman and Dawson, 1996), rooting strategies are complex and highly species-specific (Demir et al., 2024). In this context, our results highlight the middle soil layer (10–30 cm) as the most reactive and significant for sustaining

transpiration, with anomaly magnitudes nearly twice those of both the upper (0–10 cm) and deep (30–60 cm) layers across all forest types.

In addition, seasonal comparisons revealed that summer soil moisture anomalies were more negative than those in spring for all forest types (Fig. S12). This is likely linked to higher temperatures and evapotranspiration during summer, which intensify water stress and drive seasonal variation in soil moisture availability. Forest density and rooting characteristics substantially influenced the relative magnitude of soil moisture anomalies (Figs. S13 and S14, respectively). Denser forests exhibited stronger negative anomalies during dry periods and enhanced positive anomalies in wet periods, amplifying seasonal fluctuations. For example, high-density (LAI scaling factor 1.6) conifer stands showed relative anomalies up to 25 % greater than their low-density counterparts (Fig. S14). In contrast, shallow-rooted systems moderated this response, leading to more stable soil moisture dynamics. Among the management scenarios, agroforestry consistently exhibited the smallest anomalies, reflecting greater buffering capacity and higher ecohydrological resilience.

The improved rooting scheme in EcoPlot-iso represents depth-dependent transpiration by dynamically linking root water uptake efficiency to soil moisture availability across three soil compartments (see Sect. 3.2). The implemented formulation enables transpiration demand to be partitioned across soil layers according to rooting distribution and soil moisture availability within a parsimonious conceptual framework. The aim was not to optimize species-specific root dynamics, but to represent the relative influence of rooting depth on water uptake and partitioning, particularly in shallow-rooted or structurally diverse systems such as young forests. While the new implementation improves the process representation of root–soil interactions, it did not result in a substantial improvement in simulated soil moisture. For shallow vegetation types such as grasslands and croplands, model performance – measured using the mKGE was similar with and without the new transpiration function (results not shown). Moreover, direct validation of the root uptake scheme remains challenging due to the lack of supporting observations, such as root distribution data, xylem water isotopes, or sap flux measurements. Addressing this issue is a clear priority for future research.

These findings highlight how structurally diverse systems, such as agroforests, can buffer drought impacts by improving groundwater recharge and reducing the amplitude of soil moisture fluctuations (Tetzlaff et al., 2024). Together, these insights underscore the importance of rooting depth, forest structure, and seasonal climate variability in shaping soil moisture patterns and regulating vegetation water use. Accounting for these factors is essential for informing adaptive forest management in drought-sensitive catchments like the DMC.

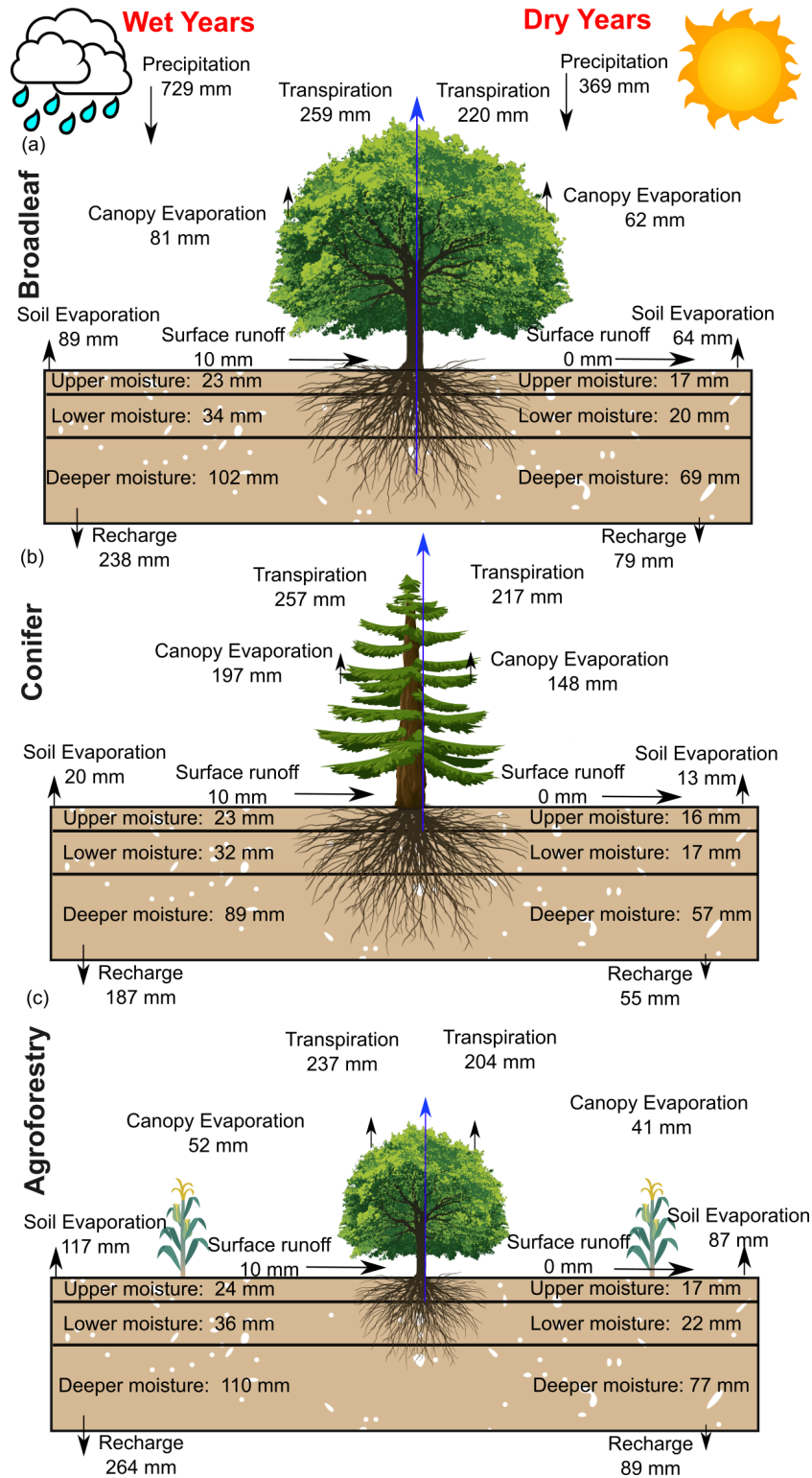


Figure 12. Comparison of mean annual water fluxes and soil moisture in the upper, middle, and deep layers for broadleaf (a), coniferous (b), and agroforestry (c) forests under dry (2006, 2018, 2022) and wet (2002, 2007, 2010, 2023) year conditions.

5.3 Advancing Tracer-Aided Ecohydrological Modelling: Challenges and Future Outlook

This study demonstrates that tracer-aided ecohydrological models, such as the isotope-aided EcoPlot-iso, can be used to effectively quantify the impact of forest management scenarios on water partitioning and ecohydrological resilience. By distinguishing between evaporation, transpiration, and subsurface water movements using stable isotopes (Soulsby et al., 2015), the model captures key hydrological responses – including evapotranspiration (ET), groundwater recharge, and soil moisture dynamics – under varying management strategies. These insights support evidence-based decision-making in drought-sensitive landscapes.

Despite these advances, several challenges remain. Conducted in a 66 km² mid-sized basin, this study did not include land use change induced atmospheric feedbacks – such as changes in albedo, radiative balance, or rainfall patterns – which are less critical at this scale but become important in larger-scale modeling (Ellison et al., 2012; Filoso et al., 2017). Moreover, this study applied a multi-objective calibration approach, combined with Monte Carlo sampling, that equally weighted isotopic and soil moisture data. However, further investigation is needed into how these observational constraints are balanced and interpreted. Recent advances – such as the DREAM(LoAX) framework (Wu et al., 2025) – demonstrate how simultaneous calibration and diagnostic analysis under the equifinality thesis can improve parameter identifiability, model robustness, and process understanding in tracer-aided ecohydrological models.

While this study used $\delta^2\text{H}$ to constrain evaporative fractionation given, the combined use of $\delta^{18}\text{O}$ and $\delta^2\text{H}$ (or d-excess) may help improve the separation of evaporation effects and mixing processes (e.g. Penna et al., 2018) though this was beyond the scope of this paper. Many recent studies have used isotopic data to investigate root water uptake patterns, revealing how tree species, soil properties, and spatial water availability shape plant water use strategies (Demir et al., 2024; Rothfuss and Javaux, 2017). Integrating tracer-aided models with soil and xylem water isotope data offers a promising path to improving the representation of root water uptake, which is often simplified in current modelling approaches (Birkel et al., 2025). Improving root uptake representation requires consideration of species-specific traits and local soil-water conditions. However, the practical application of such improvements is limited by the scarcity of soil and xylem water isotope data, which are essential for constraining root water uptake dynamics but remain rare due to the labor-intensive and technically demanding nature of field sampling and laboratory analysis (Landgraf et al., 2022; Sprenger et al., 2017). This scarcity hinders the spatial and temporal resolution of observational data, limiting our ability to refine root water uptake processes in tracer-aided models.

Upscaling from plot to landscape level remains complex due to spatial heterogeneity in vegetation, soils, and topogra-

phy. Addressing this requires spatially distributed modeling frameworks that can explicitly capture heterogeneity in ecohydrological processes across different landscape units (van Huijgevoort et al., 2016; Kuppel et al., 2018). Enhanced integration with remote sensing techniques can also help address these scaling limitations by providing spatially continuous data on vegetation dynamics, soil moisture, and ET (Yang et al., 2023). Incorporating ET observations, for instance, could strengthen model interpretation of flux dynamics. Currently, key processes such as lateral subsurface flows and upward capillary fluxes are not explicitly represented in the EcoPlot-iso model. Including these components, along with improved representation of groundwater-surface water interactions, could improve simulations of hydrological connectivity and water storage dynamics.

It is important to note that the scenario framework presented here is intentionally exploratory and management-oriented, rather than species-specific. While EcoPlot-iso captures key controls on water partitioning through canopy structure, soil moisture dynamics, and tracer-based separation of fluxes, additional physiological traits – such as stomatal regulation, vapor pressure deficit (VPD) sensitivity, and species-specific drought stress strategies – are not explicitly represented. These processes are known to influence transpiration dynamics and vegetation responses to drought, and their inclusion represents an important direction for future model development. Accordingly, the results of this study are interpreted in a relative sense, emphasizing comparative responses and management-relevant trade-offs rather than absolute or species-level predictions.

6 Conclusion and Outlook

The tracer-aided ecohydrological model EcoPlot-iso was applied to quantify how alternative forest management scenarios influence long-term water partitioning and ecohydrological resilience in the drought-sensitive Demnitzer Millcreek catchment (DMC), northeastern Germany. Baseline simulations for the period 2000–2024 were established at three forest sites (broadleaf forest, conifer forest, and agroforestry) and successfully reproduced observed soil moisture and soil water isotope ($\delta^2\text{H}$) dynamics through a multi-criteria calibration approach. A key development in this study was the integration of a depth-dependent root water uptake function, which enable the representation of transpiration across soil layers associated with contrasting rooting distributions and stand ages. Building on these baseline simulations, a generic scenario framework was applied to systematically assess the effects of forest type, forest density, and rooting characteristics on evapotranspiration, groundwater recharge, and soil moisture dynamics under contrasting dry and wet climatic conditions.

The results revealed clear trade-offs between evapotranspiration (ET) and groundwater recharge across different for-

est management scenarios. On average, conifer forest exhibited higher ET, approximately 7%–11% greater than broadleaf forest and agroforestry, accompanied by reduced groundwater recharge, particularly during low-flow periods. In contrast, agroforestry buffered drought stress, maintained lower soil moisture variability, and enhanced groundwater recharge. Conifers showed the strongest soil moisture anomalies, indicating greater drought sensitivity, while agroforests exhibited the most stable soil water storage. The middle soil layer (10–30 cm) was identified as the most responsive zone, consistently exhibiting the largest anomalies due to its role as the dominant root water uptake region supporting transpiration.

Beyond advancing process understanding, this study provided a practical and transferable framework for land management. By incorporating key controls such as canopy properties and root distribution, EcoPlot-iso facilitates an accessible means of assessing long-term land management impacts on landscape ecohydrology. The visualization and decision-support framework developed here offers a transparent, scenario-based platform for evaluating forest management strategies in climate-sensitive regions. These tools are well-suited for informing resilient land use planning under increasing climate variability.

Looking ahead, future research could usefully aim to incorporate additional isotopic tracers – such as deeper soil water (> 1 m), groundwater, and xylem water isotopes – to further constrain root water uptake functions and capture their variability across species and hydroclimatic conditions. The integration of high-resolution remote sensing data – particularly LiDAR for detailed characterization of forest structure – will enhance model parameterization and improve the spatial representation of heterogeneity in canopy height, leaf area distribution, and forest density. Advancing the EcoPlot-iso framework to incorporate lateral subsurface flows, groundwater dynamics, and coupled land–atmosphere feedbacks will support broader applications, including the assessment of large-scale land use change. Collectively, these developments will enhance model robustness and enable more informed, resilient land and water management strategies under a warming climate.

Code and data availability. The data and code that support the findings of this study are available from the corresponding author upon reasonable request.

Supplement. The supplement related to this article is available online at <https://doi.org/10.5194/hess-30-3715-2026-supplement>.

Author contributions. CJ contributed to the methodology, software development, formal analysis, investigation, visualization, and writing of the original draft. DT contributed to conceptualization, inves-

tigation, data curation, validation, resources, project administration, and funding acquisition. SW contributed to methodology, investigation and data curation. CB contributed to software, methodology, and resources. HL contributed to investigation, visualization and validation. CS contributed to conceptualization, methodology, validation, investigation. All authors contributed to writing – review and editing.

Competing interests. The contact author has declared that none of the authors has any competing interests.

Disclaimer. Publisher's note: Copernicus Publications remains neutral with regard to jurisdictional claims made in the text, published maps, institutional affiliations, or any other geographical representation in this paper. The authors bear the ultimate responsibility for providing appropriate place names. Views expressed in the text are those of the authors and do not necessarily reflect the views of the publisher.

Acknowledgements. Tetzlaff's contributions were partly funded through the WETSCAPES2.0 project (DFG TRR410/1 2025). Tetzlaff also received funding from the “Wasserressourcenpreis 2024” awarded by the Rüdiger Kurt Bode-Foundation. Contributions from Soulsby were supported by Leibniz Association Germany in the project Wetland Restoration in Peatlands. Laudon was funded by KAW 2018.0259 and 2023.0245, and Soulsby was also funded as an International KSLA Guest Professor at SLU by the Wallenberg Foundation (WP2023-0001). Birkel would like to thank the IGB for generously supporting him with a senior fellowship and the UCR for a sabbatical license. We extend our appreciation to Benedikt Boesel and the team from the Finck Foundation (<https://www.finck-stiftung.org>, last access: 15 June 2026) for their collaborative support and for granting access to study sites. The authors are very grateful for the constructive comments provided by the Editor, Prof. Dr. Anke Hildebrandt, and two anonymous reviewers.

Financial support. This research has been supported by the Deutsche Forschungsgemeinschaft (grant no. TRR410/1 2025) and the Knut och Alice Wallenbergs Stiftelse (grant nos. WP2023-0001, 2018.0259, and 2023.0245).

Review statement. This paper was edited by Anke Hildebrandt and reviewed by two anonymous referees.

References

- Ault, T. R.: On the essentials of drought in a changing climate, *Science*, 368, 256–260, <https://doi.org/10.1126/science.aaz5492>, 2020.
- Birkel, C., Arciniega-Esparza, S., Maneta, M. P., Boll, J., Stevenson, J. L., Benegas-Negri, L., Tetzlaff, D., and

- Soulsby, C.: Importance of measured transpiration fluxes for modelled ecohydrological partitioning in a tropical agroforestry system, *Agric. For. Meteorol.*, 346, <https://doi.org/10.1016/j.agrformet.2023.109870>, 2024.
- Birkel, C., Tetzlaff, D., Ring, A. M., and Soulsby, C.: Does high resolution in situ xylem and atmospheric vapor isotope data help improve modeled estimates of ecohydrological partitioning?, *Agr. Forest Meteorol.*, 365, <https://doi.org/10.1016/j.agrformet.2025.110467>, 2025.
- Bonan, G. B.: Forests and climate change: Forcings, feedbacks, and the climate benefits of forests, *Science*, 320, 1444–1449, <https://doi.org/10.1126/science.1155121>, 2008.
- Bosch, J. M. and Hewlett, J. D.: A review of catchment experiments to determine the effect of vegetation changes on water yield and evapotranspiration, *J. Hydrol.*, 55, 3–23, [https://doi.org/10.1016/0022-1694\(82\)90117-2](https://doi.org/10.1016/0022-1694(82)90117-2), 1982.
- Brauman, K. A., Freyberg, D. L., and Daily, G. C.: Forest structure influences on rainfall partitioning and cloud interception: A comparison of native forest sites in Kona, Hawai'i, *Agr. Forest Meteorol.*, 150, <https://doi.org/10.1016/j.agrformet.2009.11.011>, 2010.
- Brown, A. E., Zhang, L., McMahon, T. A., Western, A. W., and Vertessy, R. A.: A review of paired catchment studies for determining changes in water yield resulting from alterations in vegetation, *J. Hydrol.*, 310, 28–61, <https://doi.org/10.1016/j.jhydrol.2004.12.010>, 2005.
- Brown, A. E., Western, A. W., McMahon, T. A., and Zhang, L.: Impact of forest cover changes on annual streamflow and flow duration curves, *J. Hydrol.*, 483, <https://doi.org/10.1016/j.jhydrol.2012.12.031>, 2013.
- Calder, I. R.: Water use by forests, limits and controls, *Tree Physiol.*, 18, 625–631, <https://doi.org/10.1093/treephys/18.8-9.625>, 1998.
- Davies-Barnard, T., Valdes, P. J., Jones, C. D., and Singarayer, J. S.: Sensitivity of a coupled climate model to canopy interception capacity, *Clim. Dyn.*, 42, 1715–1732, <https://doi.org/10.1007/s00382-014-2100-1>, 2014.
- Demir, G., Guswa, A. J., Filipzik, J., Metzger, J. C., Römermann, C., and Hildebrandt, A.: Root water uptake patterns are controlled by tree species interactions and soil water variability, *Hydrol. Earth Syst. Sci.*, 28, 1441–1461, <https://doi.org/10.5194/hess-28-1441-2024>, 2024.
- Ellison, D., Futter, M. N., and Bishop, K.: On the forest cover-water yield debate: From demand- to supply-side thinking, *Glob. Change Biol.*, 18, <https://doi.org/10.1111/j.1365-2486.2011.02589.x>, 2012.
- Emerman, S. H. and Dawson, T. E.: Hydraulic lift and its influence on the water content of the rhizosphere: An example from sugar maple, *Acer saccharum*, *Oecologia*, 108, <https://doi.org/10.1007/BF00334651>, 1996.
- Estrela, T. and Vargas, E.: Drought Management Plans in the European Union. The Case of Spain, *Water Resour. Manag.*, 26, 1537–1553, <https://doi.org/10.1007/s11269-011-9971-2>, 2012.
- Evaristo, J. and McDonnell, J. J.: Prevalence and magnitude of groundwater use by vegetation: A global stable isotope meta-analysis, *Sci. Rep.*, 7, <https://doi.org/10.1038/srep44110>, 2017.
- Falkenmark, M. and Rockström, J.: The New Blue and Green Water Paradigm: Breaking New Ground for Water Resources Planning and Management, *J. Water Resour. Plan. Manag.*, 132, [https://doi.org/10.1061/\(asce\)0733-9496\(2006\)132:3\(129\)](https://doi.org/10.1061/(asce)0733-9496(2006)132:3(129)), 2006.
- Faticchi, S., Ivanov, V. Y., and Caporali, E.: A mechanistic ecohydrological model to investigate complex interactions in cold and warm water-controlled environments: 1. Theoretical framework and plot-scale analysis, *J. Adv. Model. Earth Syst.*, 4, <https://doi.org/10.1029/2011MS000086>, 2012.
- Filoso, S., Bezerra, M. O., Weiss, K. C. B., and Palmer, M. A.: Impacts of forest restoration on water yield: A systematic review, *PLoS One*, 12, <https://doi.org/10.1371/journal.pone.0183210>, 2017.
- Gelbrecht, J., Driescher, E., Lademann, H., Schönfelder, J., and Exner, H.-J.: Diffuse nutrient impact on surface water bodies and its abatement by restoration measures in a small catchment area in North-East Germany, *Water Sci. Technol.*, 33, <https://doi.org/10.2166/wst.1996.0501>, 1996.
- Gelbrecht, J., Lengsfeld, H., Pöthig, R., and Opitz, D.: Temporal and spatial variation of phosphorus input, retention and loss in a small catchment of NE Germany, *J. Hydrol.*, 304, 151–165, <https://doi.org/10.1016/j.jhydrol.2004.07.028>, 2005.
- Geris, J., Tetzlaff, D., McDonnell, J., and Soulsby, C.: The relative role of soil type and tree cover on water storage and transmission in northern headwater catchments, *Hydrol. Process.*, 29, <https://doi.org/10.1002/hyp.10289>, 2015.
- Gigante, V., Iacobellis, V., Manfreda, S., Milella, P., and Portoghese, I.: Influences of Leaf Area Index estimations on water balance modeling in a Mediterranean semi-arid basin, *Nat. Hazards Earth Syst. Sci.*, 9, 979–991, <https://doi.org/10.5194/nhess-9-979-2009>, 2009.
- Guswa, A. J., Tetzlaff, D., Selker, J. S., Carlyle-Moses, D. E., Boyer, E. W., Bruen, M., Cayuela, C., Creed, I. F., van de Giesen, N., Grasso, D., Hannah, D. M., Hudson, J. E., Hudson, S. A., Iida, S., Jackson, R. B., Katul, G. G., Kumagai, T., Llorens, P., Lopes Ribeiro, F., Michalzik, B., Nanko, K., Oster, C., Pataki, D. E., Peters, C. A., Rinaldo, A., Sanchez Carretero, D., Trifunovic, B., Zalewski, M., Haagsma, M., and Levina, D. F.: Advancing ecohydrology in the 21st century: A convergence of opportunities, *Ecohydrology*, 13, e2208, <https://doi.org/10.1002/eco.2208>, 2020.
- Hersbach, H., Bell, B., Berrisford, P., Hirahara, S., Horányi, A., Muñoz-Sabater, J., Nicolas, J., Peubey, C., Radu, R., Schepers, D., Simmons, A., Soci, C., Abdalla, S., Abellan, X., Balsamo, G., Bechtold, P., Biavati, G., Bidlot, J., Bonavita, M., De Chiara, G., Dahlgren, P., Dee, D., Diamantakis, M., Dragani, R., Flemming, J., Forbes, R., Fuentes, M., Geer, A., Haimberger, L., Healy, S., Hogan, R. J., Hólm, E., Janisková, M., Keeley, S., Laloyaux, P., Lopez, P., Lupu, C., Radnoti, G., de Rosnay, P., Rozum, I., Vamborg, F., Villaume, S., and Thépaut, J.-N.: The ERA5 global reanalysis, *Q. J. Roy. Meteorol. Soc.*, 146, 1999–2049, <https://doi.org/10.1002/qj.3803>, 2020.
- Hibbert, A. R.: Forest treatment effects on water yield, in: *International Symposium on Forest Hydrology*, edited by: Sopper, W. E. and Lull, H. W., Pergamon Press, Oxford, UK, 527–543, 1967.
- Huntington, T. G.: Evidence for intensification of the global water cycle: Review and synthesis, *J. Hydrol.*, 319, 83–95, <https://doi.org/10.1016/j.jhydrol.2005.07.003>, 2006.
- Kleine, L., Tetzlaff, D., Smith, A., Dubbert, M., and Soulsby, C.: Modelling ecohydrological feedbacks in forest and grassland plots under a prolonged drought anomaly

- in Central Europe 2018–2020, *Hydrol. Process.*, 35, <https://doi.org/10.1002/hyp.14325>, 2021.
- Kling, H., Fuchs, M., and Paulin, M.: Runoff conditions in the upper Danube basin under an ensemble of climate change scenarios, *J. Hydrol.*, 424–425, <https://doi.org/10.1016/j.jhydrol.2012.01.011>, 2012.
- Kool, D., Agam, N., Lazarovitch, N., Heitman, J. L., Sauer, T. J., and Ben-Gal, A.: A review of approaches for evapotranspiration partitioning, *Agr. Forest Meteorol.*, 184, 56–70, <https://doi.org/10.1016/j.agrformet.2013.09.003>, 2014.
- Kuppel, S., Tetzlaff, D., Maneta, M. P., and Soulsby, C.: ECH2O iso 1.0: Water isotopes and age tracking in a process-based, distributed ecohydrological model, *Geosci. Model Dev.*, 11, 3045–3069, <https://doi.org/10.5194/gmd-11-3045-2018>, 2018.
- Landgraf, J., Tetzlaff, D., Wu, S., Freymüller, J., and Soulsby, C.: Using stable water isotopes to understand ecohydrological partitioning under contrasting land uses in a drought-sensitive rural, lowland catchment, *Hydrol. Process.*, 36, e14779, <https://doi.org/10.1002/hyp.14779>, 2022.
- Landgraf, J., Tetzlaff, D., Birkel, C., Stevenson, J. L., and Soulsby, C.: Assessing land use effects on ecohydrological partitioning in the critical zone through isotope-aided modelling, *Earth Surf. Process. Landf.*, 48, 3199–3219, <https://doi.org/10.1002/esp.5691>, 2023.
- Larcher, W.: *Physiological Plant Ecology*, Springer-Verlag, New York, 1975.
- Leuschner, C., Voß, S., Foetzki, A., and Clases, Y.: Variation in leaf area index and stand leaf mass of European beech across gradients of soil acidity and precipitation, *Plant Ecol.*, 186, <https://doi.org/10.1007/s11258-006-9127-2>, 2006.
- Li, K. Y., Boisvert, J. B., and De Jong, R.: An exponential root-water-uptake model, *Can. J. Soil Sci.*, 79, <https://doi.org/10.4141/S98-032>, 1999.
- Llorens, P. and Domingo, F.: Rainfall partitioning by vegetation under Mediterranean conditions, A review of studies in Europe, *J. Hydrol.*, 335, <https://doi.org/10.1016/j.jhydrol.2006.10.032>, 2007.
- Luo, S., Tetzlaff, D., Smith, A., and Soulsby, C.: Assessing impacts of alternative land use strategies on water partitioning, storage and ages in drought-sensitive lowland catchments using tracer-aided ecohydrological modelling, *Hydrol. Process.*, 38, <https://doi.org/10.1002/hyp.15126>, 2024.
- Mahmood, R., Pielke, R. A., Hubbard, K. G., Niyogi, D., Dirmeyer, P. A., McAlpine, C., Carleton, A. M., Hale, R., Gameda, S., Beltrán-Przekurat, A., Baker, B., Mcnider, R., Legates, D. R., Shepherd, M., Du, J., Blanken, P. D., Frauenfeld, O. W., Nair, U. S., and Fall, S.: Land cover changes and their biogeophysical effects on climate, *Int. J. Climatol.*, 34, <https://doi.org/10.1002/joc.3736>, 2014.
- McKay, M. D., Beckman, R. J., and Conover, W. J.: Comparison of three methods for selecting values of input variables in the analysis of output from a computer code, *Technometrics*, 21, <https://doi.org/10.1080/00401706.1979.10489755>, 1979.
- Neill, A. J., Birkel, C., Maneta, M. P., Tetzlaff, D., and Soulsby, C.: Structural changes to forests during regeneration affect water flux partitioning, water ages and hydrological connectivity: Insights from tracer-aided ecohydrological modelling, *Hydrol. Earth Syst. Sci.*, 25, 4861–4886, <https://doi.org/10.5194/hess-25-4861-2021>, 2021.
- Orth, R. and Destouni, G.: Drought reduces blue-water fluxes more strongly than green-water fluxes in Europe, *Nat. Commun.*, 9, <https://doi.org/10.1038/s41467-018-06013-7>, 2018.
- Penna, D., Hopp, L., Scandellari, F., Allen, S. T., Benettin, P., Beyer, M., Geris, J., Klaus, J., Marshall, J. D., Schwendenmann, L., Volkmann, T. H. M., von Freyberg, J., Amin, A., Ceperley, N., Engel, M., Frentress, J., Giambastiani, Y., McDonnell, J. J., Zuecco, G., Llorens, P., Siegwolf, R. T. W., Dawson, T. E., and Kirchner, J. W.: Ideas and perspectives: Tracing terrestrial ecosystem water fluxes using hydrogen and oxygen stable isotopes – challenges and opportunities from an interdisciplinary perspective, *Biogeosciences*, 15, 6399–6415, <https://doi.org/10.5194/bg-15-6399-2018>, 2018.
- Pielke, R. A., Pitman, A., Niyogi, D., Mahmood, R., McAlpine, C., Hossain, F., Goldewijk, K. K., Nair, U., Betts, R., Fall, S., Reichstein, M., Kabat, P., and de Noblet, N.: Land use/land cover changes and climate: Modeling analysis and observational evidence, *WIREs Climate Change*, 2, 828–850, <https://doi.org/10.1002/wcc.144>, 2011.
- Quandt, A., Neufeldt, H., and Gorman, K.: Climate change adaptation through agroforestry: opportunities and gaps, *Curr. Opin. Environ. Sustain.*, 60, 101244, <https://doi.org/10.1016/j.cosust.2022.101244>, 2023.
- Ricci, G. F., De Girolamo, A. M., and Gentile, F.: Modeling the Effect of Different Management Practices for Soil Erosion Control in a Mediterranean Watershed, *Lecture Notes in Civil Engineering*, 67, 125–132, https://doi.org/10.1007/978-3-030-39299-4_14, 2020.
- Rothfuss, Y. and Javaux, M.: Reviews and syntheses: Isotopic approaches to quantify root water uptake: a review and comparison of methods, *Biogeosciences*, 14, 2199–2224, <https://doi.org/10.5194/bg-14-2199-2017>, 2017.
- Shen, H., Tolson, B. A., and Mai, J.: Time to Update the Split-Sample Approach in Hydrological Model Calibration, *Water Resour. Res.*, 58, <https://doi.org/10.1029/2021WR031523>, 2022.
- Smith, A., Tetzlaff, D., Gelbrecht, J., Kleine, L., and Soulsby, C.: Riparian wetland rehabilitation and beaver re-colonization impacts on hydrological processes and water quality in a lowland agricultural catchment, *Sci. Total Environ.*, 699, <https://doi.org/10.1016/j.scitotenv.2019.134302>, 2020.
- Smith, A., Tetzlaff, D., Kleine, L., Maneta, M., and Soulsby, C.: Quantifying the effects of land use and model scale on water partitioning and water ages using tracer-aided ecohydrological models, *Hydrol. Earth Syst. Sci.*, 25, 2239–2259, <https://doi.org/10.5194/hess-25-2239-2021>, 2021.
- Soulsby, C., Birkel, C., Geris, J., Dick, J., Tunaley, C., and Tetzlaff, D.: Stream water age distributions controlled by storage dynamics and nonlinear hydrologic connectivity: Modeling with high-resolution isotope data, *Water Resour. Res.*, 51, <https://doi.org/10.1002/2015WR017888>, 2015.
- Sprenger, M., Tetzlaff, D., and Soulsby, C.: Soil water stable isotopes reveal evaporation dynamics at the soil–plant–atmosphere interface of the critical zone, *Hydrol. Earth Syst. Sci.*, 21, 3839–3858, <https://doi.org/10.5194/hess-21-3839-2017>, 2017.
- Staelens, J., De Schrijver, A., Verheyen, K., and Verhoest, N. E. C.: Rainfall partitioning into throughfall, stemflow, and interception within a single beech (*Fagus sylvatica* L.) canopy: Influence of foliation, rain event characteristics, and meteorology, *Hydrol. Process.*, 22, <https://doi.org/10.1002/hyp.6610>, 2008.

- Sterling, S. M., Ducharme, A., and Polcher, J.: The impact of global land-cover change on the terrestrial water cycle, *Nat. Clim. Change*, 3, <https://doi.org/10.1038/nclimate1690>, 2013.
- Stevenson, J. L., Birkel, C., Comte, J. C., Tetzlaff, D., Marx, C., Neill, A., Maneta, M., Boll, J., and Soulsby, C.: Quantifying heterogeneity in ecohydrological partitioning in urban green spaces through the integration of empirical and modelling approaches, *Environ. Monit. Assess.*, 195, <https://doi.org/10.1007/s10661-023-11055-6>, 2023.
- Tague, C. L. and Band, L. E.: RHESSys: Regional Hydro-Ecologic Simulation System – An Object-Oriented Approach to Spatially Distributed Modeling of Carbon, Water, and Nutrient Cycling, *Earth Interact.*, 8, [https://doi.org/10.1175/1087-3562\(2004\)8<1:rrhss>2.0.co;2](https://doi.org/10.1175/1087-3562(2004)8<1:rrhss>2.0.co;2), 2004.
- Tetzlaff, D., Carey, S. K., McNamara, J. P., Laudon, H., and Soulsby, C.: The essential value of long-term experimental data for hydrology and water management, *Water Resour. Res.*, 53, 2598–2604, <https://doi.org/10.1002/2017WR020838>, 2017.
- Tetzlaff, D., Laudon, H., Luo, S., and Soulsby, C.: Ecohydrological resilience and the landscape water storage continuum in droughts, *Nat. Water*, 2, 915–918, <https://doi.org/10.1038/s44221-024-00300-y>, 2024.
- te Wierik, S. A., Cammeraat, E. L. H., Gupta, J., and Artzy-Randrup, Y. A.: Reviewing the Impact of Land Use and Land-Use Change on Moisture Recycling and Precipitation Patterns, *Water Resour. Res.*, 57, <https://doi.org/10.1029/2020WR029234>, 2021.
- Trenberth, K. E.: Changes in precipitation with climate change, *Clim. Res.*, 47, 123–138, <https://doi.org/10.3354/cr00953>, 2011.
- van Huijgevoort, M. H. J., Tetzlaff, D., Sutanudjaja, E. H., and Soulsby, C.: Using high resolution tracer data to constrain water storage, flux and age estimates in a spatially distributed rainfall-runoff model, *Hydrol. Process.*, 30, 4761–4778, <https://doi.org/10.1002/hyp.10902>, 2016.
- Wang-Erlandsson, L., van der Ent, R. J., Gordon, L. J., and Savenije, H. H. G.: Contrasting roles of interception and transpiration in the hydrological cycle – Part 1: Temporal characteristics over land, *Earth Syst. Dynam.*, 5, 441–469, <https://doi.org/10.5194/esd-5-441-2014>, 2014.
- Wu, J., Zhang, R., and Gui, S.: Modeling soil water movement with water uptake by roots, *Plant Soil*, 215, <https://doi.org/10.1023/A:1004702807951>, 1999.
- Wu, S., Tetzlaff, D., Goldammer, T., and Soulsby, C.: Hydroclimatic variability and riparian wetland restoration control the hydrology and nutrient fluxes in a lowland agricultural catchment, *J. Hydrol.*, 603, <https://doi.org/10.1016/j.jhydrol.2021.126904>, 2021.
- Wu, S., Tetzlaff, D., Yang, X., Smith, A., and Soulsby, C.: Integrating Tracers and Soft Data Into Multi-Criteria Calibration: Implications From Distributed Modeling in a Riparian Wetland, *Water Resour. Res.*, 59, <https://doi.org/10.1029/2023WR035509>, 2023.
- Wu, S., Tetzlaff, D., Beven, K., and Soulsby, C.: DREAM(LoAX): Simultaneous Calibration and Diagnosis for Tracer-Aided Ecohydrological Models Under the Equifinality Thesis, *Water Resour. Res.*, 61, e2024WR038779, <https://doi.org/10.1029/2024WR038779>, 2025.
- Yang, X., Tetzlaff, D., Müller, C., Knöller, K., Borchardt, D., and Soulsby, C.: Upscaling Tracer-Aided Ecohydrological Modeling to Larger Catchments: Implications for Process Representation and Heterogeneity in Landscape Organization, *Water Resour. Res.*, 59, <https://doi.org/10.1029/2022WR033033>, 2023.
- Ying, Z., Tetzlaff, D., Comte, J.-C., Wu, S., and Soulsby, C.: Storage Dynamics and Groundwater–Surface Water Interactions in a Drought Sensitive Lowland Catchment: Process-Based Modelling as a Learning Tool, *Hydrol. Process.*, 39, e70141, <https://doi.org/10.1002/hyp.70141>, 2025.
- Yuan, X., Wang, Y., Ji, P., Wu, P., Sheffield, J., and Otkin, J. A.: A global transition to flash droughts under climate change, *Science*, 380, <https://doi.org/10.1126/science.abn6301>, 2023.
- Zhang, L., Dawes, W. R., and Walker, G. R.: Response of mean annual evapotranspiration to vegetation changes at catchment scale, *Water Resour. Res.*, 37, <https://doi.org/10.1029/2000WR900325>, 2001.
- Zhong, F., Jiang, S., van Dijk, A. I. J. M., Ren, L., Schellekens, J., and Miralles, D. G.: Revisiting large-scale interception patterns constrained by a synthesis of global experimental data, *Hydrol. Earth Syst. Sci.*, 26, 5647–5667, <https://doi.org/10.5194/hess-26-5647-2022>, 2022.